

Transient trapping into metastable states in systems with competing orders

Zhiyuan Sun¹ and Andrew J. Millis^{1,2}

¹*Department of Physics, Columbia University, 538 West 120th Street, New York, New York 10027, USA*

²*Center for Computational Quantum Physics, The Flatiron Institute, 162 5th Avenue, New York, New York 10010, USA*

(Dated: May 17, 2022)

The quench dynamics of a system involving two competing orders is investigated using a Ginzburg-Landau theory with relaxational dynamics. We consider the scenario where a pump rapidly heats the system to a high temperature, after which the system cools down to its equilibrium temperature. We study the evolution of the order parameter amplitude and fluctuations in the resulting time dependent free energy landscape. Exponentially growing thermal fluctuations dominate the dynamics. The system typically evolves into the phase associated with the faster-relaxing order parameter, even if it is not the global free energy minimum. This theory offers a natural explanation for the widespread experimental observation that metastable states may be induced by laser induced collapse of a dominant equilibrium order parameter.

I. INTRODUCTION

Dynamical phase transitions [1–3], in which systems are tuned through a phase transition by time variation of system parameters, are a fundamental topic of longstanding interest in many areas of science. For example, it is believed that cosmological expansion tuned the universe through the electroweak symmetry breaking transition [4]. Supercooled liquids are a widely studied terrestrial example. Spinodal decomposition [5–8] and Kibble-Zurek (KZ) [9–12] theories have addressed important aspects of dynamical phase transition physics for systems characterized by an order parameter which is tuned through a first or second order transition respectively.

Systems with multiple competing or intertwined orders are of great current interest in condensed matter physics [13, 14]. Examples include high T_c cuprates and transition metal dicalcogenides in which superconductivity and spin and/or charge density wave order compete and coexist as well as ‘colossal’ magnetoresistance manganites where ferromagnetic metal and charge ordered antiferromagnetic insulating states compete at low temperatures [15, 16]. Recent developments in “ultrafast” experimental technique [17–27] have made it possible to dynamically suppress one or more order parameters and study the subsequent evolution, raising the possibility of “steering” the order parameters into a desired metastable state.

The purpose of this paper is to provide theoretical insight into dynamical phase transitions in systems with multiple order parameters and in particular to draw attention to the crucial importance of the relative magnitudes of order parameter relaxation rates. We consider systems in which the relevant degrees of freedom are space-time dependent order parameter fields $\psi_i(\mathbf{r}, t)$ defined from a fundamental theory by integrating out microscopic degrees of freedom such as electrons. For notational simplicity we deal here with a system with two real order parameters. Adding more real order parameters or making the order parameters complex does not alter our conclusions.

We consider two broad classes of behavior described by the equilibrium free energy landscapes sketched in Fig. 1 (a) strictly *competing orders*, where the free energy has two lo-

cal minima, such that in each minimum only one of the two order parameters is nonzero, and Fig. 6 *intertwined order* parameters, where at the global minimum both order parameters are nonzero, but a metastable minimum exists in which only one of the order parameters is nonzero. When such systems are exposed to an experimentally relevant pump pulse they may be driven to a point in phase space near the origin (o) as indicated by the solid line trajectory in Fig. 1(a). We show that after the pump is turned off, the time evolution is dominated by the exponential amplification of very long wavelength fluctuations of the order parameters, and that even a modest difference in relaxation rates will drive the system to the minimum related to the faster evolving order, even if it is not the global free energy minimum. The probability of trapping into this metastable state is close to unity. The probability of going back to the equilibrium order

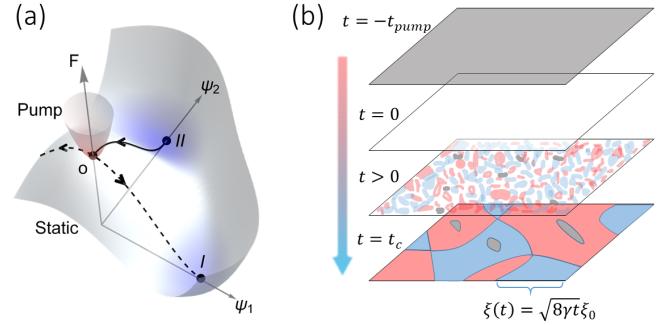


FIG. 1. (a) Equilibrium free energy landscape for two competing order parameters ψ_1 and ψ_2 . The energy is represented both as a height and with color, with lower energy appearing bluer. The point labeled II is a global free energy minimum and the point I is a locally stable minimum. The surface labeled ‘Pump’ is a free energy landscape with only one minimum, at the origin, corresponding to a high temperature state established by a pump pulse. The pump destroys order II as shown by the black solid trajectory. In the subsequent cooling process, exponential growth of thermal fluctuations leads the system into order I , as shown by the dashed trajectory. (b) The real space illustration of order parameter evolution in the fast cooling limit. Gray means order II and blue/red means positive/negative order I . Large domains are formed at time t_c with only a small volume fraction being the original order II .

scales as $p_2 \sim \zeta^\delta$ where $\zeta \ll 1$ is the same Ginzburg parameter that controls the validity of static mean field theory and δ is a positive number defined later. Nucleation dynamics operating on much longer time scales will lead eventually to relaxation to the global minimum [1, 28], but this physics is not explicitly considered here.

Transient dynamics in systems with a single order parameter have been extensively discussed; the literature is too large to review here but we note that a recent study of a quench to the superconducting state has derived from microscopics the model A dynamics used here [29]. Transient dynamics in systems with competing orders has been previously discussed in terms of deterministic dynamics of spatially uniform order parameters [30–32]. Our paper goes beyond the previous work by studying the formation and growth of spatial fluctuations and focusing on the difference in order parameter time constants.

Section II describes the physical picture and defines the formalism. Section C has the general solution to the dynamical problem. Section IV discusses the fast cooling limit which illustrates the essential physics. Section V analyzes the effect of slower cooling rate. Section VI discusses systems with intertwined orders. Section VII contains detailed comparison to recent experiments. Section VIII is a summary and conclusion, containing a discussion of the assumptions made and consequences of relaxing them. Appendices give detailed derivations of some of the formulas in the main text.

II. PHYSICAL PICTURE AND FORMALISM

We consider a system in which the important degrees of freedom are space-time dependent order parameter fields $\psi_i(\mathbf{r}, t)$ obtained from a fundamental theory by integrating out quasiparticles. We assume that the order parameter fields evolve according to dissipative [relaxational Time-Dependent-Ginzburg-Landau (TDGL) or “Model A”] dynamics [1, 29, 33, 34] defined by a free energy functional F which is time dependent because of the applied pump field:

$$\frac{1}{\gamma_i} \partial_t \psi_i(\mathbf{r}, t) = -\frac{1}{E_c} \frac{\delta F(t)}{\delta \psi_i(\mathbf{r}, t)} + \eta_i(\mathbf{r}, t). \quad (1)$$

Here γ_i are the corresponding relaxation rates, E_c is the condensation energy density and η is a noise field determined by the microscopic degrees of freedom that were integrated out to obtain the order parameter theory. The free energy functionals are assumed to be of the general form

$$F[\psi_1, \psi_2] = E_c \int d^D \mathbf{r} (f_1 + f_2 + f_c), \quad (2)$$

$$f_i = -\alpha_i \psi_i^2 + (\xi_{i0} \nabla \psi_i)^2 + \psi_i^4$$

as sketched in Fig. 1(a). Here the ξ_{i0} are the bare coherence lengths, D is the spatial dimension and

$$f_c = c \psi_1^2 \psi_2^2 \quad (3)$$

describes the interaction between the two order parameters in the competing order case.

In our convention, ψ_i , α_i , c and f_i are dimensionless, intensive and defined such that the quartic term in the free energy has coefficient 1 and the α_i are of the order of unity at zero temperature. For cooperation ($c < 0$) or weak competition ($0 < c < 2$), F has a single minimum. For $c > 2$, F has two locally stable minima if α_1 and $\alpha_2 > 0$ and $\frac{2}{c} < \frac{\alpha_1}{\alpha_2} < \frac{c}{2}$ (see Appendix A). We study the $c > 2$ (multiple minima) case in this paper. Following usual practice we assume that all parameters are temperature independent except the $\alpha_i = \kappa_i(T_{ci} - T)/T_{ci}$, which are positive at low temperatures, negative at high temperatures, vary smoothly with temperature and vanish at the respective critical temperatures $T = T_{ci}$ (we assume linear temperature dependence for simplicity). The nonequilibrium enters the formalism as a time dependence of the α_i , determined by the time dependence of the effective temperature $T(t)$ of the microscopic degrees of freedom that were integrated out. We focus on the case $\alpha_2 > \alpha_1$ but $\gamma_2 \alpha_2 < \gamma_1 \alpha_1$ so minimum II is the equilibrium free energy minimum but the dynamics associated with minimum I is faster.

The condensation energy density E_c , in combination with ξ_{i0} , sets the relevant microscopic scales. An important dimensionless measure of the thermal fluctuations is

$$G_i(T) = \frac{T}{E_c \xi_{i0}^D}. \quad (4)$$

The Ginzburg parameter defined in the conventional theory of critical phenomena is $G(T_c) \alpha^{\frac{D-4}{2}}$ with mean field theory applying when the parameter is much less than unity. For example, in the weak coupling case of conventional superconductors, $G \sim (\text{gap/fermi energy})^{D-1}$. The treatment that follows is formally valid in the $G \ll 1$ limit.

The stochastic Eq. (1) may be recast as a Fokker-Planck equation for a probability functional $\rho[\{\psi_k\}]$ that gives the distribution of fluctuations around the mean field value (see, e.g., [1, 35, 36] and Appendix B). In the linearized approximation used below the probability functional is a direct product $\rho[\psi] = \prod_k \rho_k(\psi_k)$ where

$$\rho_k = \frac{1}{\sqrt{2\pi D_k(t)}} e^{-\frac{\psi_k^2}{2D_k(t)}} \quad (5)$$

is a Gaussian distribution for each Fourier mode ψ_k of the field with time-dependent variance $D_k(t) = \langle \psi_k(t) \psi_{-k}(t) \rangle$ which we calculate below.

We are primarily interested in understanding experiments in which a system is highly excited by a pump pulse and the subsequent evolution is probed. We assume that the pump does not couple directly to the order parameters; rather, it excites microscopic degrees of freedom (e.g. electron quasiparticles or phonons) which thermalize very quickly (relative to the order parameter timescales) to a quasiequilibrium state described by an effective temperature $T(t)$ [37]. The effective temperature is maintained by the pump at a high value T_H for some time. After the pump is turned off, $T(t)$

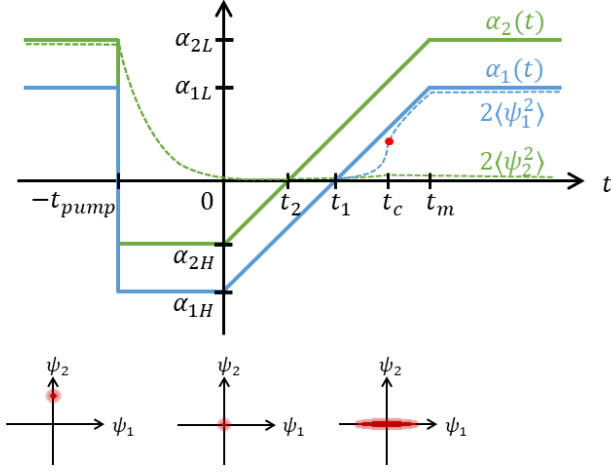


FIG. 2. Upper panel: time evolution of quadratic free energy coefficients $\alpha_i(t)$ (solid lines) and mean square values of order parameters (dashed lines). Different colors denote different orders. The pump maintains the system at a high temperature T_H (negative $\alpha = \alpha_{iH}$) for the time $-t_{\text{pump}} < t < 0$, after which the temperature relaxes to the equilibrium one T_L (positive $\alpha = \alpha_{iL}$) over a time t_m . Shown is the linear cooling profile used to derive exact formulas in the slow cooling case. The mean field order parameter is suppressed during the high temperature stage. Order parameter fluctuation $\langle \psi_i(r)^2 \rangle$ starts to grow exponentially after t_i , as shown by the dashed curves. The red dot denotes the point of crossover to nonlinear dynamics ($\langle \psi_1^2 \rangle \sim \alpha_1(t)$) at time t_c . Lower panel: the local order parameter probability distributions $\rho(\psi_1, \psi_2)$ corresponding to the time intervals vertically above.

evolves over a timescale t_m to the true thermal equilibrium temperature T_L determined by the bath. In most experiments, the bath is the lattice and t_m is just the electron-phonon thermalization time scale which is typically of the order of picoseconds. This assumption is in essence the two temperature model of Rothwarf and Taylor [38] in which one set of degrees of freedom (e.g., electrons or a particular set of phonon modes) is excited to a high temperature and then relaxes back to the equilibrium temperature set by the rest of the system.

Within these assumptions, the instantaneous value of $T(t)$ determines the parameters α_i of the free energy and the noise. We take the noise correlators

$$\langle \eta_i(\mathbf{r}, t) \eta_i(\mathbf{r}', t') \rangle = \frac{2T(t)}{\gamma_i E_c} \delta(\mathbf{r} - \mathbf{r}', t - t') \quad (6)$$

to be local in space and time and consistent with the fluctuation-dissipation theorem. Here the Boltzmann constant k_B is set to unity and the average is over a probability distribution of the noise field. For the slow dynamics we consider here, the relevant frequency/momentum scale is well below those of the microscopic degrees of freedom that are integrated out, justifying the locality assumption of Eq. (6).

Representative time histories of $\alpha(t)$ are shown in Fig. 2. There are three time regimes: (a) *pump on*, covering the time interval $-t_{\text{pump}} < t < 0$ in which the temperature $T = T_H$

and correspondingly the quadratic coefficient $\alpha = \alpha_H < 0$; (b) *relaxation*, time $0 < t < t_m$, during which T evolves from T_H through T_c to T_L while α evolves from $\alpha_H < 0$ through $\alpha = 0$ to $\alpha_L > 0$; and (c) *evolution*, time $t > t_m$, $T = T_L$ and $\alpha = \alpha_L$. It is convenient also to introduce the time $t_0 = \frac{T_H - T_c}{T_H - T_L} t_m$, at which $T = T_c$ and $\alpha(t) = 0$ (the t_0 times for order parameters ψ_1 and ψ_2 are labeled as t_1 and t_2 in Fig. 2).

The physical picture is that for $t \in (-t_{\text{pump}}, t_0)$, the free energy landscape has its only minimum at $\psi = 0$ (point O in Fig. 1(a)). Thus the high temperature produced by the pump suppresses the mean field order parameter to nearly zero and the fluctuations remain bounded. After time t_0 , point O becomes unstable, the long wavelength fluctuations start to grow exponentially with time and the correlation length grows as $\xi \sim \xi_0 \sqrt{8\gamma t}$. This process leads to the creation of large domains where most domains are in phase I as shown in Fig. 1(b).

III. DYNAMICS

In this section we present a general solution of Eq. (1) with time dependent α and noise correlators as described above. The initial condition is

$$\psi(\mathbf{r})^{\text{init}} = \bar{\psi} + \sum_{\mathbf{k}} e^{i\mathbf{k}\cdot\mathbf{r}} \delta\psi_{\mathbf{k}} \equiv \bar{\psi} + V \int \frac{d^D k}{(2\pi)^D} e^{i\mathbf{k}\cdot\mathbf{r}} \delta\psi_{\mathbf{k}} \quad (7)$$

where $\bar{\psi}$ is the initial order parameter, $\delta\psi_{\mathbf{k}}$ represents thermal fluctuations about the initial ordered state and V is the system volume. For simplicity of notation, here and henceforth we suppress the index i labelling the different order parameters wherever possible. In the initial state, fluctuations are assumed small: $\bar{\psi}^2 \gg \langle \delta\psi(r=0)^2 \rangle \equiv \sum_{\mathbf{k}} \langle \delta\psi_{\mathbf{k}} \delta\psi_{-\mathbf{k}} \rangle \sim G$. The pump acts to decrease $\bar{\psi}^2$ and increase the fluctuations. If $\bar{\psi}^2$ remains large compared to the mean square fluctuation amplitude, the state of the system is determined by a straightforward deterministic dynamics. This case is discussed briefly below, but our main interest is in situations in which the pump drives the initial order parameter to a value smaller than the root mean square fluctuation amplitude and the physics is determined by the evolution of the fluctuations.

Because Eq. (1) is first order in time it has no “memory”, so the evolution over one time regime fixes initial conditions for the next one. We will first consider the evolution over the decaying order parameter regime $t < t_0$; the resulting state of the system at t_0 is then the initial condition for the subsequent evolution.

In the pump-on regime the system is hot (temperature $T = T_H$) so the free energy is dominated by a large quadratic term which justifies the use of linearized dynamics even when the order parameter is not small. This means that in the pump-on regime we may study

$$\frac{1}{\gamma} \partial_t \psi_{\mathbf{k}} = 2\alpha_{\mathbf{k}}(t) \psi_{\mathbf{k}} + \eta_{\mathbf{k}} \quad (8)$$

where

$$\alpha_k(t) = \alpha(t) - \xi_0^2 k^2 < 0. \quad (9)$$

We assume that the dynamics in the pump-on regime drives the order parameter to a small enough value that we may continue to use the linearized approximation throughout the $t < t_0$ regime and for some time into the growing fluctuations ($t > t_0$) regime. Conditions for the validity of this approximation will be presented below. The solution of Eq. (8) may be written as

$$\psi_k(t) = \psi_k^{init} e^{S_k(t, -t_{pump})} + \gamma \int_{-t_{pump}}^t dt' \eta_k(t') e^{S_k(t, t')} \quad (10)$$

where the first term gives the propagation forward in time of the initial order parameter $\psi_k^{init} = \bar{\psi} \delta_{k,0} + \delta\psi_k$ with mean field part $\bar{\psi}$ and small fluctuations $\delta\psi$. The second term represents the propagation forward of fluctuations created by the noise after $-t_{pump}$. The accumulated phase S is defined as

$$S_k(t_a, t_b) = 2\gamma \int_{t_b}^{t_a} dt \alpha_k(t) \quad (11)$$

and $S_0(t_a, t_b)$ has the interpretation as the signed area enclosed by the solid lines and the time axis in Fig. 2. With Eq. (6), the square of Eq. (10) yields the fluctuation amplitude

$$D_k(t) = D_k^{init} e^{2S_k(t, -t_{pump})} + \frac{2\gamma}{E_c V} \int_{-t_{pump}}^t dt' T(t') e^{2S_k(t, t')} \quad (12)$$

defined in Eq. (5) where D_k^{init} is the initial fluctuation amplitude.

In the linear cooling profile approximation the initial mean field order parameter amplitude evolves as

$$\bar{\psi}(t_0) = e^{-|\alpha_H| \gamma t_0} e^{-2|\alpha_H| \gamma t_{pump}} \bar{\psi} \quad (13)$$

where the factor $e^{-2|\alpha_H| \gamma t_{pump}}$ gives the exponential suppression during the pump-on stage and the $e^{-|\alpha_H| \gamma t_0}$ factor gives the additional suppression during $t \in (0, t_0)$. We assume that $|\alpha_H| \gamma (2t_{pump} + t_0)$ is large enough that the mean field order parameter is reduced to a very small value at $t = t_0$, less than the mean square fluctuations. As shown in detail in section V, this assumption plus a small Ginzburg parameter implies that at time t_0 , the system is well prepared in a disordered state with negligible mean field order parameter and small fluctuations.

We now consider the evolution of the distribution at times after t_0 , where the system has cooled below the transition temperature ($\alpha(t) > 0$) so long wavelength modes with $k < \sqrt{\alpha} \xi_0^{-1}$ grow exponentially with time. As long as the fluctuation does not become too large the linearized equation may be used for the dynamics so

$$D_k(t) = e^{2S_0(t, t_0) - 4k^2 \xi_0^2 \gamma (t - t_0)} \left(D_k(t_0) + \frac{2\gamma}{E_c V} \int_{t_0}^t dt' e^{-2S_k(t', t_0)} T(t') \right) \quad (14)$$

where as before the first term represents the propagation forward in time of the fluctuations existing at t_0 while the second term represents the additional contributions generated by the noise thereafter. A detailed analysis given in Appendix C shows that the second term in Eq. (14) is of the same order as the first in the situations of interest here.

The key observation is that long wavelength modes with $4\xi_0^2 k^2 \gamma (t - t_0) < 2S_0(t, t_0)$ are exponentially amplified and we are interested in long times $\gamma(t - t_0) \gg 1$ for which the growth is substantial ($e^{2S_0(t, t_0)} \sim G^{-1}$). The exponential growth continues until the local mean square fluctuation amplitude of one of the order parameters becomes large enough that the nonlinearity becomes important to the dynamics, i.e., until t reaches the crossover time t_c defined by

$$\langle \psi_i(r=0)^2 \rangle_{t=t_c} \sim \alpha_i / 2. \quad (15)$$

To compute $\langle \psi_i(0)^2 \rangle$ we observe that at long times the important momentum dependence is controlled by the $e^{-4k^2 \xi_0^2 \gamma (t - t_0)}$ factor. Defining the time-dependent correlation length by

$$\xi^2(t) = \xi_0^2 (8\gamma(t - t_0) + 1/a) \quad (16)$$

we perform the momentum integral to obtain (up to an unimportant overall factor) the correlation function in real space

$$\begin{aligned} \langle \psi(0) \psi(r) \rangle_t &= V \int \frac{d^D k}{(2\pi)^D} D_k(t) e^{i\mathbf{k} \cdot \mathbf{r}} \\ &= \frac{G/a}{(16\pi\gamma(t - t_0))^{\frac{D}{2}}} e^{2S_0(t, t_0)} e^{-\frac{r^2}{2\xi(t)^2}}. \end{aligned} \quad (17)$$

The details of the pump and initial cooling enter Eq. (16) and (17) via the a which varies from $\sim \alpha_L$ in the fast cooling limit to α_{KZ} in the slow cooling case (to be discussed in Sec. V). This variation leads to corrections that are subleading relative to the terms we consider and we will not explicitly notate this dependence henceforth.

Eqs. (17) is the first key result. The exponential factors show that the fluctuations grow exponentially in time, and the spatial correlation is governed by the universal correlation length growth law $\xi \sim \xi_0 \sqrt{8\gamma t}$ which does not depend on the equilibrium value of α or temperature-time profile.

IV. FAST COOLING LIMIT

In this section we consider the fast cooling limit $t_m \rightarrow 0$ which illustrates the essential physics with minimal complexity. In the fast cooling limit the phase for the exponential amplification term in Eq. (17) is simply

$$2S_0(t, t_0) = 4\alpha_L \gamma t \quad (18)$$

and Eq. (15) for the crossover time t_c is

$$4\alpha_L \gamma t_c = \ln \frac{1}{\zeta} + \frac{D}{2} \ln(4\alpha_L \gamma t_c) \quad (19)$$

where we have set a in Eq. (17) to α_L without altering the leading behavior, and have defined

$$\zeta = 2(4\pi)^{-\frac{D}{2}} \alpha_L^{D/2-2} G \quad (20)$$

which is in effect the usual Ginzburg parameter of the theory of critical phenomena. Similar results were previously presented by Lemonik and Mitra [39] who noted the importance of the Ginzburg parameter in setting post-quench timescales. We see that t_c is logarithmically large if ζ is small, i.e. if mean field theory works well for equilibrium. At time t_c of the fast order I , the fluctuation of the slow order II is smaller by the ratio

$$\frac{\langle \psi_2^2 \rangle}{\langle \psi_1^2 \rangle} = \frac{\alpha_{1L}}{\alpha_{2L}} \left(\frac{\gamma_1}{\gamma_2} \right)^{D/2} \frac{G_2}{G_1} \left(\frac{1}{\zeta_1} \left(\ln \frac{1}{\zeta_1} \right)^{D/2} \right)^{\frac{\alpha_{2L}\gamma_2}{\alpha_{1L}\gamma_1} - 1} \quad (21)$$

which is much less than unity if $\gamma_2 \alpha_{2L} < \gamma_1 \alpha_{1L}$ and $\zeta \ll 1$. At this stage of the evolution the two order parameters are independent and the joint distribution of local amplitudes at a position r is the product of Gaussians:

$$\rho(\psi_1(r), \psi_2(r)) = \frac{\text{Exp} \left[-\frac{\psi_1^2}{2\langle \psi_1^2 \rangle} - \frac{\psi_2^2}{2\langle \psi_2^2 \rangle} \right]}{2\pi \sqrt{\langle \psi_1^2 \rangle \langle \psi_2^2 \rangle}}. \quad (22)$$

For $\gamma_2 \alpha_{2L} < \gamma_1 \alpha_{1L}$ the mean square values are very different, leading to the highly anisotropic joint distribution function shown in Fig. 3(a)(c). The probability distribution describing the space dependence of the fluctuations is derived in Appendix H and is plotted in Fig. 3(b)(d) for order I . We see that the fluctuations of order parameter I are highly correlated over scales out to $\xi(t) \gg \xi_0$ (the fluctuations of the slower order parameter II are correlated over slightly shorter distances).

Thus the physical picture at $t = t_c$ is of order parameter domains of typical size $\xi(t_c) \approx \sqrt{\ln \frac{1}{\zeta}} \sqrt{\frac{2}{\alpha_L}} \xi_0 \gg \xi_0$ within which the order parameters are nearly uniform and normally distributed and with the typical value of ψ_1 much larger than ψ_2 , as illustrated in Fig. 1(b). Moreover, the typical value of local ψ is now much larger than the new fluctuation scale induced by the noise, so that in the subsequent evolution the mean field dynamics dominates over the effect of the noise. Therefore, to study the subsequent evolution it suffices to consider the evolution within a domain, which is described by the uniform, deterministic TDGL equations, written here for the competing orders case:

$$\begin{aligned} \gamma_1^{-1} \partial_t \psi_1 &= 2\alpha_1 \psi_1 - 4\psi_1^3 - 2c\psi_2^2 \psi_1, \\ \gamma_2^{-1} \partial_t \psi_2 &= 2\alpha_2 \psi_2 - 4\psi_2^3 - 2c\psi_1^2 \psi_2 \end{aligned} \quad (23)$$

with initial conditions chosen from the joint probability distribution $\rho(\psi_1(0), \psi_2(0))$. The issues associated with matching the solutions at the domain walls are a coarsening problem discussed briefly below.

The flow defined by Eq. (23) has a simple phase space structure with stable fixed points defined by the minima of

F , as shown in Fig. 4. Each initial condition defines a trajectory that flows into one of the minima. For the physically relevant case $\alpha_{1L}, \alpha_{2L} > 0$ with $\frac{2}{c} < \frac{\alpha_{1L}}{\alpha_{2L}} < \frac{c}{2}$ there are four fixed points, with basins of attraction separated by a four-branched separatrix curve. We may estimate the position of the separatrix by matching the small ψ regime, where the exponential growth requires

$$\psi_1 = \lambda \psi_2^{1/\Delta} \quad (24)$$

to the requirement that the separatrix goes through the saddle point $(\psi_1^2, \psi_2^2) = (c\alpha_{2L} - 2\alpha_{1L}, c\alpha_{1L} - 2\alpha_{2L})/(c^2 - 4)$. Here $\Delta = \gamma_2 \alpha_{2L} / \gamma_1 \alpha_{1L} < 1$ and the coefficient is fixed by the matching condition.

By finding the relative weights of the probability distribution in the different basins of attraction we can estimate the relative volume fractions of the different order parameter domains. The volume fraction p_2 of order II domains is just the probability of (ψ_1, ψ_2) lying in the basin of attraction of minimum II in Fig. 4, which at time $t = t_c$ can be

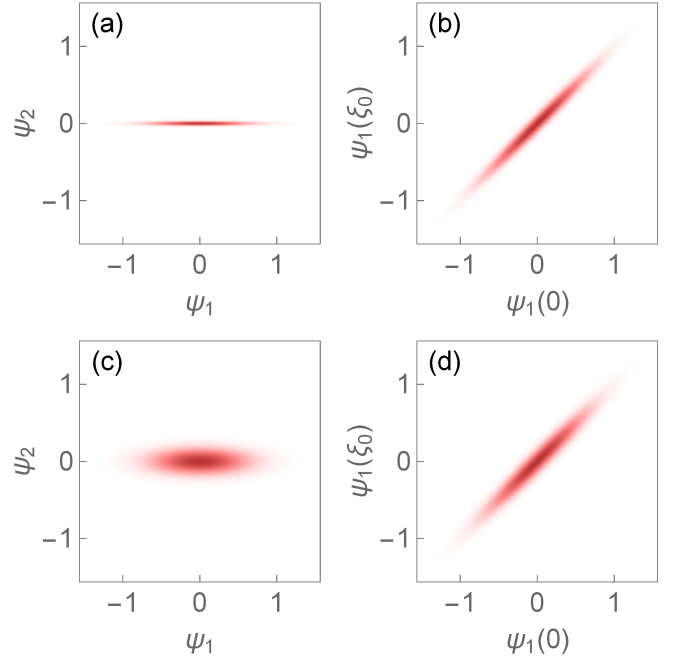


FIG. 3. Panel (a)(c) are the density plots of the Gaussian probability distribution $\rho(\psi_1(r), \psi_2(r))$ computed at time $t = 2.0$ ps for $G_1 = G_2 = 10^{-5}$ (panel (a)) and $t = 1.0$ ps for $G_1 = G_2 = 10^{-2}$ (panel (c)) in the fast cooling limit $t_m = 0$. Regions of higher value of ρ appear redder. Panel (b)(d) show the two point probability $\rho(\psi_1(0), \psi_1(\xi_0))$ distributions for the same two cases. The common parameters used are $(\alpha_{1L}, \alpha_{2L}) = (1.0, 1.1)$, $(\gamma_1, \gamma_2) = (2, 1) \text{ ps}^{-1}$, $\xi_0 = \xi_0$ and $D = 3$.

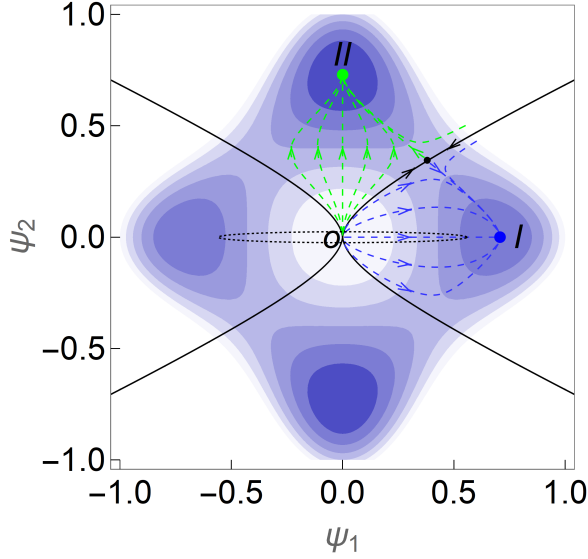


FIG. 4. Basins of attraction of the two orders on the contour plot of the free energy landscape. Lower energy appears bluer. The arrows show the direction of order parameter dynamics. Black solid line separates the basins. The parameters used are $(\alpha_{1L}, \alpha_{2L}) = (1.0, 1.1)$, $(\gamma_1, \gamma_2) = (2, 1) \text{ ps}^{-1}$ and $c = 6$. Black dotted line illustrates the magnitudes of ψ_i fluctuations at time $t = 2.0 \text{ ps}$ for $G_1 = G_2 = 10^{-4}$ and spatial dimension $D = 3$. Most of the probability lies in the basin of order I meaning most volume of the system will be trapped into I afterwards.

estimated as

$$\begin{aligned}
 p_2 &\approx 4 \int_0^\infty d\psi_2 \rho(\psi_1 = 0, \psi_2) \lambda \psi_2^{1/\Delta} \\
 &= \frac{1}{\pi} 2^{\frac{1}{2\Delta} + \frac{1}{2}} \Gamma\left(\frac{1}{2}\left(1 + \frac{1}{\Delta}\right)\right) \lambda \langle \psi_1^2 \rangle^{\frac{1/\Delta - 1}{2}} \left(\frac{\langle \psi_2^2 \rangle}{\langle \psi_1^2 \rangle}\right)^{\frac{1}{2\Delta}} \\
 &= \vartheta \left(\ln \frac{1}{\zeta_1}\right)^{-\frac{\delta}{2}} \zeta_1^\delta
 \end{aligned} \tag{25}$$

where $\delta = (1/\Delta - 1)/2 > 0$ and $\vartheta \sim 1$ can be found in Appendix I. Thus the proportion of ψ_2 domains is suppressed by a power law of the Ginzburg parameter $\zeta \ll 1$ and is negligibly small even if the time scales are just slightly different. Eq. (25) is the second key result of this paper.

Life time of the metastable state—Each domain then evolves to the appropriate minimum; the evolution takes a time of the order of $\frac{1}{\alpha_L \gamma} \ln \frac{1}{\zeta}$, after which the physical picture is of a set of domains, most of which have $\psi_1 = \pm \sqrt{\alpha_{1L}/2}$ and $\psi_2 \approx 0$ (i.e. are in phase I) while a small volume fraction of the sample are phase II domains where $\psi_2 = \pm \sqrt{\alpha_{2L}/2}$ and $\psi_1 \approx 0$, as illustrated in Fig. 1(b). However, long range order is not established. The subsequent evolution is determined by spontaneous nucleation of phase II regions in the dominant phase I domains, and by growth of the existing ψ_2 domains. The timescale for ultimate equilibration thus depends both on nucleation rates and on domain wall dynamics, both of which are beyond the scope of this paper. We do, however, provide a likely lower limit on the equilibration

time by considering the free growth of ψ_2 domains, assuming no domain wall pinning and nucleation which is an exponentially slow process. The speed of domain wall motion is at the order of $v \sim \gamma \xi_0$ as long as the free energy difference δf between the two minima is order one. Assuming the phase II domains are evenly distributed among the phase I domains we can estimate the equilibration time as

$$t_{life} \sim \left(\frac{1}{p_2}\right)^{\frac{1}{D}} \xi(t_c)/v \sim \frac{1}{\gamma} \left(\ln \frac{1}{\zeta}\right)^{\frac{1}{2}(1+\delta)} \left(\frac{1}{\zeta}\right)^{\frac{\delta}{D}}. \tag{26}$$

If the order parameters are complex ones corresponding to $U(1)$ symmetry breaking, as in the case of superconductivity (SC) being order I and charge density wave (CDW) being order II , one just needs to double the degrees of freedom for each order before nonlinear dynamics is onset. As a result, Eq. (25) gives the offset of trapping probability as

$$p_2 \sim \left(\ln \frac{1}{\zeta}\right)^{-D\delta} \zeta^{2\delta} \tag{27}$$

and Eq. (26) is modified to

$$t_{life} \sim \frac{1}{\gamma} \left(\ln \frac{1}{\zeta}\right)^{\frac{1}{2}+\delta} \left(\frac{1}{\zeta}\right)^{\frac{2\delta}{D}}. \tag{28}$$

After t_c , the different SC regions are characterized by different order parameter phases which can continuously synchronize to leave behind topological vortices. The number density of the vortices scales as $n \sim 1/\xi(t_c)^2 \sim \left(\xi_0^2 \frac{2}{\alpha_L} \ln \frac{1}{\zeta}\right)^{-1}$, different from the Kibble-Zurek scaling [10] since the latter applies to the slow cooling limit.

V. FINITE COOLING RATE

We now ask how the physics is modified as the cooling time t_m is increased from zero. The essential picture derived in the previous section of long length-scale domains of one or the other order parameter still applies, but because the time t_0 of transition from exponential decay to exponential growth is earlier for order II than that for order I , the ψ_2 fluctuations will have a longer period of growth than the ψ_1 fluctuations. The longer period of growth will compensate for the faster dynamics of ψ_1 , meaning that the condition on the difference in relaxation rates required for the system to evolve to minimum I becomes more stringent. A second issue is that the cross over to nonlinear dynamics may occur at a time $t < t_m$ before the relaxation of the α to its equilibrium value is complete, meaning that the free energy landscape at the point of crossing to nonlinearity differs from the equilibrium one. For these reasons the behavior for given t_m depends on the ratio of relaxation rates γ_2/γ_1 in a somewhat complicated manner. The various regimes are shown in Fig. 5.

A. The state at t_0

We first characterize the state at $t = t_0$. If the mean field order parameter is reduced to a small value, then the thermal fluctuations existing at time $t = -t_{\text{pump}}$ (the first term in Eq. (12)) will be reduced to a completely negligible level so the order parameter at $t = t_0$ and subsequent times is determined entirely by the random noise. We distinguish *fast cooling* ($|\alpha_H|\gamma t_0 \leq 1$) and *slow cooling* ($|\alpha_H|\gamma t_0 \geq 1$) regimes according to whether the cooling to t_0 after the pump is turned off has a significant effect on the order parameter. The linearized dynamics means that the corresponding distribution function is the product of Gaussians given in Eq. (5). Averaging the solution for $\psi_k(t_0)$ over the noise using Eq. (6) shows that the fluctuation distribution half-width defined in Eq. (5) is

$$D_k(t_0) = \frac{2\gamma}{E_c V} \int_{-t_{\text{pump}}}^{t_0} dt' e^{2S_k(t_0, t')} T(t'). \quad (29)$$

The integral in Eq. (29) may easily be evaluated numerically, and in the linear quench approximation may be expressed exactly in terms of error functions (see Appendix D). Here we present results in important limits which explicate the basic physics. In the fast cooling limit the portion of the integral from $t = 0 \rightarrow t_0$ makes a negligible contribution and we find

$$D_k(t_0) \approx \frac{T_H}{2E_c V} \frac{1}{|\alpha_H| + \xi_0^2 k^2} \quad (30)$$

indicating that in the fast cooling limit the fluctuations at $t = t_0$ are those of the hot thermal state created by the pump, with distance $|\alpha_H|$ from criticality and correlation length $\xi_H = \xi_0/\sqrt{|\alpha_H|}$. In the slow cooling regime only times near t_0 are important and we find

$$D_k(t_0) \approx \frac{T_c}{E_c V} \frac{1}{\alpha_{KZ}} \int_0^\infty dv \text{Exp}[-v^2 - 2\xi_{KZ}^2 k^2 v] = \begin{cases} \frac{\sqrt{\pi}}{2\alpha_{KZ}} \frac{T_c}{E_c V}, & k \ll 1/\xi_{KZ} \\ 1/(2\xi_0^2 k^2), & k \gg 1/\xi_{KZ} \end{cases} \quad (31)$$

where the effective distance from criticality α_{KZ} and corresponding correlation length ξ_{KZ} are given by

$$\alpha_{KZ} = \sqrt{|\alpha_H|/(2\gamma t_0)}, \quad \xi_{KZ} = \xi_0/\sqrt{\alpha_{KZ}} \quad (32)$$

which depend on the square root of the cooling rate, consistent with Kibble-Zurek scaling [9, 10] and the mean field exponents of the problem at hand.

The correlation function in real space is given by

$$\langle \psi(0)\psi(r) \rangle_t = V \int^{k_c} \frac{d^D k}{(2\pi)^D} D_k(t) e^{i\mathbf{k}\cdot\mathbf{r}} \quad (33)$$

where the upper cutoff k_c which we expect to be of the order of a few times ξ_0^{-1} is required to make the integral finite as $r \rightarrow 0$. The momentum integral is dominated by large

momenta for which $D_k \sim (k\xi_0)^{-2}$, so the local fluctuation amplitude is

$$\langle \psi^2(0) \rangle_{t_0} = \begin{cases} \frac{G_{D=2}}{8\pi} \ln(1 + k_c^2 \xi^2), & (D=2) \\ \frac{G_{D=3} k_c \xi_0}{2\pi^2} \left(1 - \frac{1}{k_c \xi} \tan^{-1} k_c \xi\right), & (D=3) \end{cases} \quad (34)$$

where G (Eq. (4)) is to be evaluated at temperature $T = T_H, T_c$ in the fast and slow quench limits respectively and ξ takes the value appropriate for the relevant limit.

To summarize, if the initial pump and subsequent cooling are strong enough to drive the initial mean field order parameter to a level smaller than the local root mean square fluctuation then at time $t = t_0$ the order parameter fluctuations in both the rapid and slow quench cases are described by a Gaussian (mean field-like) probability characterized by a temperature (T_H or T_c), a distance from criticality ($|\alpha_H|$ or α_{KZ}) and the associated correlation length $\xi_{H,KZ}^2 = \xi_0^2/\alpha_{H,KZ}$. The local mean square local fluctuation order parameters are of the order of G , justifying Eq. (17) even in the slow cooling case. Using Eqs. (13) and (34) we see the criterion for suppression of the mean field order parameter is roughly $|\alpha_H|\gamma(2t_{\text{pump}} + t_0) \gg \ln(1/G)$. The linearized analysis used here requires that $\langle \psi^2(r=0) \rangle \ll \alpha$. A renormalization group-improved treatment will break down when $G\alpha(t) \frac{D-4}{2} \sim 1$ (the Ginzburg criterion) which sets an upper limit on the cooling time $t_m \sim \zeta^{-1/(1-D/4)}/\gamma \equiv t_{mc}$ in the slow quench regime.

It is important to remember that the T_c (and thus t_0) of the two different order parameters are different as are the bare correlation lengths and relaxation constants, so especially in the slow cooling limit the probability distribution functions of the two order parameters will differ, especially at long wavelengths, although Eq. (34) shows that the local fluctuation amplitudes, which are determined by short wavelength fluctuations, are not too different for the two order parameters.

B. The trapping condition

Now we analyze the effect of finite cooling rate on the condition for trapping into phase I . To simplify the formulas, in the main text we focus on the exponential growth and neglect power-law prefactors, thus approximating $\langle \psi^2 \rangle_t \sim G e^{2S(t, t_0)}$. Our main focus will be on establishing how small γ_2 must be relative to γ_1 for the system to evolve with high probability into the metastable minimum I . We will find dependence of the critical ratio $\Delta = \frac{\gamma_2 \alpha_{I2}}{\gamma_1 \alpha_{L1}}$ is a scaling function of the variable t_m/t_{mu} , where t_{mu} is the cooling time at which the onset of nonlinearity t_c coincides with the equilibration time t_m .

To begin the analysis we note that for $t_m > 0$ and $t > t_m$ the accumulated phase becomes (after eliminating t_0 in favor of α_L)

$$2S_0(t, t_0) = 4\alpha_L \gamma \left(t - \frac{t_m}{2} \frac{2|\alpha_H| + \alpha_L}{|\alpha_H| + \alpha_L} \right) \quad (35)$$

and Eq. (19) for the crossover time becomes

$$t_c = \frac{t_m}{2} \frac{2|\alpha_H| + \alpha_L}{|\alpha_H| + \alpha_L} + \frac{1}{4\gamma\alpha_L} \ln \frac{1}{\zeta} \quad (36)$$

while Eq. (21) becomes

$$\frac{\langle \psi_2^2 \rangle}{\langle \psi_1^2 \rangle} = e^{2\alpha_{2L}\gamma_2 t_m \frac{|\alpha_{1H}|\alpha_{2L} - |\alpha_{2H}|\alpha_{1L}}{(|\alpha_{2H}| + \alpha_{2L})(|\alpha_{1H}| + \alpha_{1L})}} \left(\frac{1}{\zeta_1} \right)^{\frac{\alpha_{2L}\gamma_2}{\alpha_{1L}\gamma_1} - 1}. \quad (37)$$

The factor $(1/\zeta_1)^{\frac{\alpha_{2L}\gamma_2}{\alpha_{1L}\gamma_1} - 1}$ is Eq. (21) with only the leading term in t_c retained and the exponential factor expresses the additional growth of ψ_2 due α_2 crossing zero earlier than α_1 . When

$$t_m = \frac{|\alpha_{1H}| + \alpha_{1L}}{2\gamma_1\alpha_{1L}^2} \ln \frac{1}{\zeta_1} = \frac{1}{2\gamma_1\alpha_{1L}} \frac{T_H - T_L}{T_{c1} - T_L} \ln \frac{1}{\zeta_1} \equiv t_{mu} \quad (38)$$

we have $t_c = t_m$, i.e., the onset of nonlinearity occurs at $t = t_m$. Thus the onset of nonlinearity occurs before equilibration only for cooling rates very slow relative to the basic order parameter timescales by a factor of the order of the log of the Ginzburg parameter. Using

$$\frac{|\alpha_{1H}|\alpha_{2L} - |\alpha_{2H}|\alpha_{1L}}{(|\alpha_{2H}| + \alpha_{2L})(|\alpha_{1H}| + \alpha_{1L})} = \frac{T_{c2} - T_{c1}}{T_H - T_L} \quad (39)$$

we see that $\langle \psi_2^2 \rangle / \langle \psi_1^2 \rangle < 1$ provided that $\Delta = \alpha_{2L}\gamma_2 / (\alpha_{1L}\gamma_1)$ is less than a critical value defined by

$$\frac{1}{1 + \frac{T_{c2} - T_{c1}}{T_{c1} - T_L} \frac{t_m}{t_{mu}}} \equiv f_1 \left(\frac{t_m}{t_{mu}} \right) \quad (40)$$

as shown in Fig. 5. In the $t_m \rightarrow 0$ limit Eq. (40) reverts to the previous result $\alpha_2\gamma_2 < \alpha_1\gamma_1$ (up to logarithmic corrections), but as t_m increases the constraint on γ_2 becomes more stringent and when $t_m = t_{mu}$ Eq. (40) becomes

$$\Delta = \frac{T_{c1} - T_L}{T_{c2} - T_L} \equiv r < 1. \quad (41)$$

For $t_m > t_{mu}$, ψ_1 reaches nonlinearity before t_m which is the regime considered by Kibble-Zurek theory [10]. Note that relaxational dynamics predicts a logarithmic correction to Kibble-Zurek scaling, as described in Appendix F. In this time regime the accumulated phase may be written

$$2S_0(t, t_0) = 2\gamma \frac{\alpha_L}{t_m - t_0} (t - t_0)^2 \quad (42)$$

and after some algebra Eq. (15) for phase I can be written as

$$t_c = t_1 + (t_m - t_1) \sqrt{\frac{t_{mu}}{t_m}}. \quad (43)$$

which is obviously before t_m if $t_m > t_{mu}$. The condition $S(t_c, t_2) < S(t_c, t_1)$ becomes

$$\Delta < \frac{t_{mu}}{t_m} \frac{r}{\left(1 - r \left(1 - \sqrt{\frac{t_{mu}}{t_m}}\right)\right)^2} \equiv f_2 \left(\frac{t_m}{t_{mu}} \right) \quad (44)$$

Symbol	Physical meaning
$-t_{pump}$	When pump pulse arrives
t_0	When the temperature crosses T_c
t_1, t_2	t_0 for order I, II
t_m	Cooling (electron-phonon thermalization) time scale
t_c	The time that fluctuation becomes comparable to 1
t_{mu}	The cooling time scale that makes $t_c = t_m$ (Eq. (38))
t_{ms}	See discussion around Eq. (45)
t_{mc}	The cooling time scale where mean field theory fails
Δ	The critical ratio $\gamma_2\alpha_{L2}/(\gamma_1\alpha_{L1})$
δ	$(1/\Delta - 1)/2$

TABLE I. Physical meaning of various time scales and Δ .

which reduces to our previous Eq. (41) when $t_m = t_{mu}$ and drops as $1/t_m$ for large t_m so that as the equilibration time becomes extremely long, the system would evolve to the equilibrium minimum unless the relaxation rate γ_2 becomes exceptionally small.

Even if Eq. (44) is satisfied, the system will only evolve to the metastable minimum if α_i are such that the metastable minimum exists at the time order I crosses to nonlinearity, i.e., if $\alpha_2(t_c) < \frac{c}{2}\alpha_1(t_c)$ which yields

$$t_m < t_{mu} \frac{(T_{c1} - T_L)^2}{(T_{c2} - T_{c1})^2} \left(\frac{c}{2} \frac{\kappa_1 T_{c2}}{\kappa_2 T_{c1}} - 1 \right)^2 \equiv t_{ms}. \quad (45)$$

If $t_m > t_{ms}$, as denoted by ‘?’ in Fig. 5, the following would happen in the cooling process: at t_c , the time for ψ_1 crossing over to nonlinear dynamics, the free energy landscape has not recovered enough such that order I is not yet a local minimum. Thus trapping into the order I state won’t necessarily happen even if $\langle \psi_2^2 \rangle \ll \langle \psi_1^2 \rangle$ at this time. We see that typically t_{ms} cannot be too much larger than t_{mu} , unless either $T_{c2} - T_{c1}$ is very small or $\kappa_1 \gg \kappa_2$ or $c \gg 2$. The various time scales are collected in Table I.

Below the upper critical dimension $D = 4$, our ‘time dependent fluctuation around mean field’ approach fails if at the predicted cross over time t_c , the system is still inside the critical regime $G\alpha(t)^{\frac{D-4}{2}} \sim 1$ (the Ginzburg criterion) where even renormalization group improved treatment breaks down. This imposes an ultimate upper limit

$$t_{mc} \equiv \frac{1}{\gamma_1} \zeta^{-\frac{1}{1-D/4}} \quad (46)$$

for the cooling time, see Appendix F. This much larger time scale is deep inside the ‘?’ region and is also labeled in Fig. 5.

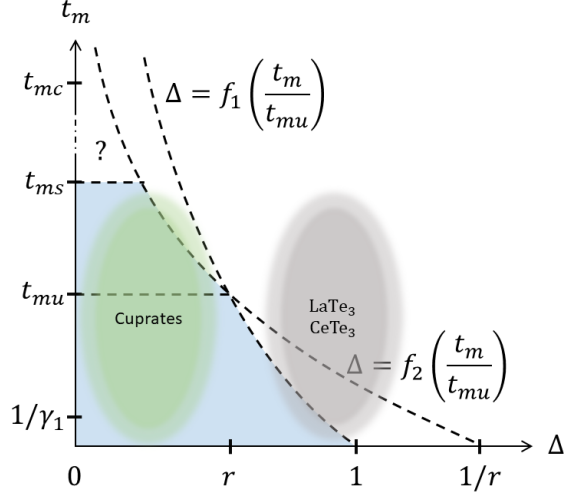


FIG. 5. A schematic ‘phase’ diagram delineating the behavior on the cooling time t_m versus $\Delta = \gamma_2 \alpha_{2L} / (\gamma_1 \alpha_{1L})$ plane. The horizontal axis can be viewed as γ_2 while all other parameters are fixed. In the blue region, trapping into phase I happens because $\langle \psi_2^2 \rangle / \langle \psi_1^2 \rangle < 1$ at t_c . The region $t_m > t_{ms}$ is unexplored in this paper and discussed in Sec. VB. The green/gray ellipses are our tentative guess of where the cuprates/rare earth tri-tellurides lie on this diagram.

VI. INTERTWINED ORDER

To study the intertwined case we modify Eq. (2) to shift one of the minima away from one of the axes. One simple choice is to add a term to f_c so

$$f_c \rightarrow c\psi_1^2\psi_2^2 + d_1\psi_1^4\psi_2^2. \quad (47)$$

and with, now, $0 < c < 2$ and $d_1 > 0$. We assume $T_{c2} > T_{c1}$ but that the difference in T_c is not too large, and d_1 is not too small. In this case (see Appendix A for details), as temperature is lowered the system first enters a phase with only $\psi_2 \neq 0$ and then at a lower temperature the phase with $\psi_1 \neq 0$, $\psi_2 = 0$ becomes locally stable although not the global minimum. At a still lower temperature the global minimum is gradually shifted to $I+II$ where a nonzero ψ_1 component appears. If we identify ψ_2 with density wave order and ψ_1 with superconductivity, this scenario may describe stripe ordered cuprates (e.g., $\text{La}_{2-x}\text{Ba}_x\text{CuO}_4$ around $x = 1/8$): the so called pair density wave (PDW) state [14]. The free energy analysis of the ψ_2/ψ_1 minimum has previously been discussed [14]; we have generalized the free energy so that it also includes a metastable phase with purely superconducting order and will argue that this generalization is needed to describe recent ultrafast experiments [23].

The considerations sketched in the previous sections carry over directly to the intertwined order case, as shown by the red line in Fig. 6. However, an additional interesting effect may occur if we relax the assumption that the pump heats up the bath appropriate to both order parameters. If the two orders couple to different microscopic degrees of freedom, then one may consider the case when only the free

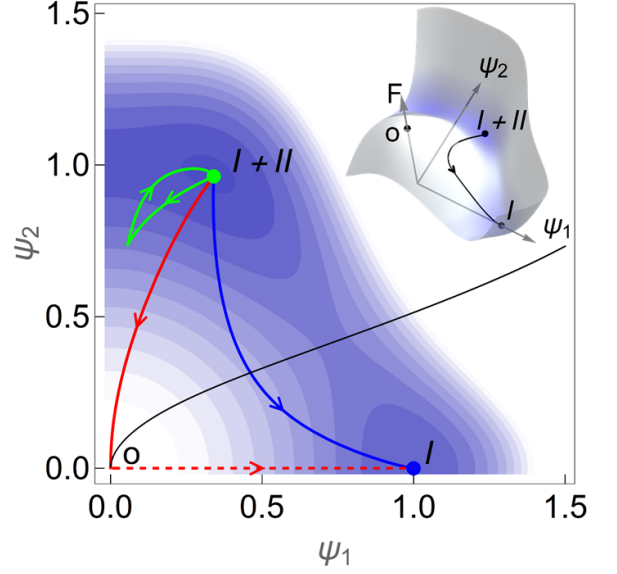


FIG. 6. Contour plot of the free energy landscape for intertwined orders. Lower energy appears bluer. The parameters used are $(\alpha_1, \alpha_2) = (2.0, 2.05)$, $(\gamma_1, \gamma_2) = (2, 1) \text{ ps}^{-1}$, $c = 1$ and $d_1 = 4$. The lines are different trajectories the system undergoes in the pump-cooling process. Red dashed line means the process is led by exponentially growing fluctuations. Thin black line is the boundary of the basin of attraction of minimum I . Inset is the free energy landscape plotted in 3D.

energy landscape for one order is changed. In particular, in the case of coupled superconducting and charge orders, one may imagine that the charge order couples to phonons much more strongly than do the electrons, so driving the phonons would affect the CDW much more strongly than the superconductivity. If the system starts in a minimum with both order parameters nonzero (as is the case for intertwined orders) and only α_2 is driven to negative, leaving α_1 positive, the transient free energy landscape will have only one minimum (I) and the mean-field dynamics will drive the system into it, as shown by the blue trajectory in Fig. 6. In this process, small fluctuations of the order parameter can be neglected and one can apply deterministic TDGL dynamics to the mean field order parameters. This mechanism does not require faster relaxation for ψ_1 ; all that is needed is that ψ_2 remains suppressed for long enough that the system evolves to the I minimum. This timescale is set by the time required for the order parameter to cross the basin boundary, $t_s \sim \frac{1}{\alpha\gamma} \ln \frac{\psi_{2m}}{\psi_{2b}}$ where ψ_{2m} is the value of ψ_2 at the original point $I+II$ and ψ_{2b} is its value at the intersection between the blue trajectory and the basin boundary. For shorter pump durations or for pumps that reduce α_1 too much, the system would relax back to the global minimum as illustrated schematically by the green trajectory in Fig. 6.

VII. EXPERIMENTS

Competing orders have been reported in many materials, and an increasing number of ultrafast experiments are appearing, including studies of competing charge density waves in tri-tellurides [25, 40], ferromagnetic domain formation in charge ordered manganites [16], and charge and magnetic order in rare earth nickelates. Much attention has focused on reports of transient superconductivity appearing in materials that have low temperature nonsuperconducting density wave states but may reasonably be expected to have competing superconducting states [18–24, 26]. The appearance of long lived superconducting-like metastable states has been seen in cuprates [18–24] through optical pump-probe by several independent groups and in FeSe through time resolved APRES [26]. This widespread mystery has heretofore been theoretically addressed via explorations of models in which the nonequilibrium drive changes the microscopic Hamiltonian, creating new physics not existing in equilibrium [41–45] and via TDGL analyses [30–32] with deterministic uniform dynamics. We argue that in many cases, the physical picture developed here is more relevant.

A. Cuprates

As an example, we consider the relevant parameters for the cuprate $\text{La}_{1.675}\text{Eu}_{0.2}\text{Sr}_{0.125}\text{CuO}_4$ (LESCO_{1/8}), the first material found to exhibit such transient phenomenon. At 10K where this compound is not superconducting due to competition of charge order, Fausti et al [18] pumped the system with a strong infrared pulse. A metastable state appeared within picoseconds and lived for at least nanoseconds. Most strikingly, it exhibits superconducting like terahertz optical response.

In discussing the application of our theory, the first issue is timescales. The timescales associated with gap recovery in cuprate superconductors are typically of the order of $\tau_{sc} \sim 1$ ps [46]; similar timescales are reported in studies of transient enhancement of the photoresponse in LESCO_{1/8} [18] and Y-Bi2212 [47]. Time resolved x-ray and electron diffraction experiments reported CDW relaxation timescales in the wide range from 4 to 1000 ps in Transition Metal Dichalcogenides (TMD) [48, 49] where the CDW order is coupled to the lattice. Timescales of only a few ps were reported for the charge order in cuprates [50], but the time scale for the stripe order that strongly competes with the superconductivity is not known, and may be long because the stripe order couples strongly to the lattice [18]. Assigning SC to order *I* and CDW to order *II*, we assume that $\tau_{sc}/\tau_{cdw} = 1/3$ for LESCO_{1/8} and $\Delta = \gamma_2\alpha_{2L}/\gamma_1\alpha_{1L} \approx 1/3$ since the $\alpha_{iL} \sim 1$ for both CDW and SC.

The next issue is the Ginsburg parameter G . The coherence lengths are of the order of a few nm and Gaussian fluctuations are observed for temperatures within 10% of T_c , so G is unlikely to be as small as it is in conventional materials. If there were no competition to CDW, the superconducting T_c of LESCO_{1/8} is about 40K, indicating a

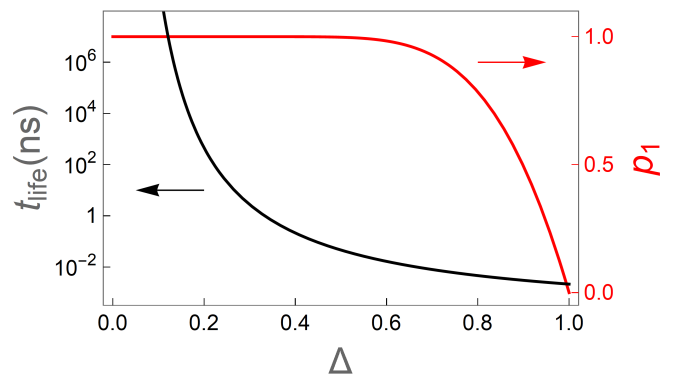


FIG. 7. The volume fraction p_1 (red curve) of SC domains and the life time t_{life} (black curve) of the metastable state as a function of $\Delta = \gamma_2\alpha_{2L}/\gamma_1\alpha_{1L}$ predicted by Eqs. (27) and (28). The Ginsburg parameter is $\zeta = 10^{-2}$.

zero temperature superconducting gap ~ 14 meV which is perhaps a factor of ~ 100 less than the Fermi energy. We suggest that $\zeta \sim G \sim 10^{-2}$ (lower panel of Fig. 3) may be appropriate since the material is effectively two dimensional.

The experiment of Fausti et al [18] could then be interpreted as destruction of both orders followed by growth of fluctuations described in section IV. The pump along a-axis had a fluence of 1 mJ/cm^2 , the penetration depth was about 200 nm and almost all the photon energy was absorbed since the reflectivity at that frequency is nearly zero. Together with the electronic specific heat of $C_{el}/T \approx 3 \text{ mJ/K}^2 \text{ mol}^{-1}$ [51] and the lattice constant of $a = 3.8 \text{ \AA}$, $c = 13.2 \text{ \AA}$ [52], we estimate that the electronic system was transiently heated up to $T_H = 2000 \text{ K}$, much larger than the critical temperatures of both CDW (80K) and SC. Thus it is reasonable to assume all orders are destroyed by the pump. The cooling time scale [18, 46] should not be significantly larger than τ_{sc} , thus the equations in the fast cooling limit should give reasonable estimations. Application of Eq. (27) in 2D yields $p_2 \approx 5 \times 10^{-6}$ as the volume fraction of CDW domains in the transient state, meaning most volume is transformed to the SC state. Eq. (28) predicts the lifetime of the metastable state to be about one nanosecond. These estimations qualitatively explain the phenomenon seen in LESCO_{1/8} but note that they depend sensitively on the values of G and Δ , see Fig. 7 and Eqs. (27) and (28).

The cuprate $\text{La}_{1.885}\text{Ba}_{0.115}\text{CuO}_4$ has a density wave transition at $T_{co} = 53 \text{ K}$ followed by a second transition at $T_c = 13 \text{ K}$ to a state with both density wave order and weak superconductivity. Cremin et al [23] recently reported that upon moderate near infrared (1.55 eV) pump pulse (fluence of 0.1 mJ/cm^2) along c-axis, the weak superconducting state may be converted to a long-lived strong superconducting like state within picoseconds. The key observation is that this state can be created only if the static system is in the weakly superconducting state below T_c of bulk superconductivity. If the static temperature is even slightly above T_c , the strong superconducting like metastable state is not created. We interpret the result as suggesting that the equilib-

rium state is an intertwined state with both superconducting and charge order, and the pump couples more strongly to the charge order while it is not strong enough to kill both orders. The transient phenomenon is due to the second mechanism described in Section VI. The transition time is $t_s \sim \frac{1}{\alpha\gamma} \ln \frac{\psi_{2m}}{\psi_{2b}} \sim \text{ps}$ if one uses $\gamma \sim 1 \text{ ps}^{-1}$. As the static temperature gets close to T_c , the transition time diverges logarithmically since ψ_{2b} approaches zero, explaining the key observation.

B. Transition metal tri-tellurides

Competing phases occur in non-superconducting contexts. In equilibrium, LaTe_3 and CeTe_3 exhibit long ranged CDW order (denoted as c-CDW). However, when these systems are driven out of equilibrium by a sufficiently strong near infrared pump, a different CDW order (denoted as a-CDW), distinguished from the equilibrium one by the wavevector, appears [40, 53]. This was interpreted as a-CDW states living in topological vortices created in the dominant cCDW state by the Kibble-Zurek mechanism. However, in the experiments by Kogar et al [40], stronger a-CDW signal was observed for a stronger pump while the Kibble-Zurek mechanism says the number of vortices depends only on the cooling time constant through T_c , a system parameter that does not quite depend on pump fluence. Our framework in section IV is an alternative explanation. Assume that the pump destroys the mean field order parameter of the c-CDW but not to zero, its recovery would suppress the growth of fluctuations of a-CDW. Therefore, a stronger pump would suppress c-CDW to a smaller value which gives more space for a-CDW fluctuations to grow. A quantitative application of our theory requires more information on the relaxation rates. Since both orders are CDWs in this case, their time scales should be comparable and we place $\text{LaTe}_3/\text{CeTe}_3$ close to $\Delta = 1$ in Fig. 5.

C. Manganites

Zhang and McLeod et al have reported that in charge ordered insulating films made of $\text{La}_{2/3}\text{Ca}_{1/3}\text{MnO}_3$ [16, 54], exposure of pump radiation can create domains of ferromagnetic metallic order, which grow in size with successive pump pulses and at low temperature, do not revert to the ground state on measureable time scales. Analysis of these experiments requires extension of our theory to the case of first order free energy landscapes.

VIII. DISCUSSION

We presented a dynamical phase transition theory of a pumped system with competing orders, based on a Landau theory of non conserved order parameters with relaxational dynamics coupled to a quasi thermal bath. We focused on the case where an applied (“pump”) field changes the free

energy landscape, thereby driving any mean field order parameters to vanishingly small values and studied in detail the growth of fluctuations after the pump is removed. We presented a general treatment valid for cooling rates that are fast or slow compared to the basic order parameter time scales, presented a scaling theory valid in the slow cooling limit, and connected our results to the Kibble-Zurek theory of systems quenched through a critical point.

We computed the probability distribution of order parameter fluctuations, identified the exponential growth of long wave length fluctuations characterized by a universal correlation length growth $\xi \sim \sqrt{8\gamma t}$, leading to a large domain structure. We showed that in physically reasonable cases, a modestly larger relaxation rate of the subdominant order can lead the system to a metastable state of domains, most of which are in this subdominant phase. We derived scaling functions for the volume fraction of different domains and the lifetime of the metastable state. Due to universality of the Landau theory, it applies to solid state systems with competing orders [18–26, 40, 47–50], cold atoms [55] and even the early universe [4].

The fluctuation theory developed here naturally explains the key features of the observations of metastable states [18, 26]: (a) the long life time ($> 200 \text{ ps}$) of the superconducting like state; (b) the finite frequency conductivity peaks [19, 56] maybe explained by the transiently created domain structure (Fig. 1(b)) which allows coupling of far field radiation to plasmonic modes. A further proof of consistency is that similar transient phenomenon are observed for both infrared and optical pumping, suggesting that the main effect of the pump is incoherent, related to heating of the microscopic degrees of freedom.

Next we discuss the assumptions underlying our approach. (a) We assume the existence of a well-defined, time-dependent temperature $T(t)$ for the high energy electronic degrees of freedom throughout the full time evolution. Indeed, quasiparticle thermalization time ($\sim 10 \text{ fs}$) is usually much shorter than the dynamics of the collective order parameter ($0.1 \sim 1 \text{ ps}$). See, e.g., Ref. [37]. Therefore, for the slow dynamics of the order parameter we consider, it is legitimate to assume a well defined temperature for high energy degrees of freedom which acts as the bath for the order parameters. (b) Our theory relies on a small Ginzburg parameter G , which is the same parameter that controls the validity of mean field theory. Thus our theory applies wherever mean field does, e.g., for SC and CDW where $\text{gap}/\text{fermi energy} \ll 1$. Although the application of mean field arguments to strongly correlated systems such as cuprates maybe questionable, our estimation using $G \sim 10^{-2}$ still renders a trapping probability close to unity. (c) We worked in the context of Ginzburg-Landau theory with relaxational dynamics which holds close to T_c [29] or for superconductors rendered gapless by magnetic impurities [33]. However, relaxational dynamics is not essential to our conclusions. If a second order time derivative is added to Eq. (1), it does not change the picture of exponential growth of the long wave length thermal fluctuations, as long as there is substantial damping to take away the energy. Extension of

our approach to the under damped (Hamiltonian dynamics) case is of interest. (d) For the trapping into the metastable order I , we need it to relax faster than the equilibrium order II . This probably happens for competing SC and CDW orders since the latter often couples to the lattice which is heavy. Since the trapping probability crosses to unity exponentially as Δ crosses one, order I just needs to be moderately faster than order II , as shown by Fig. 7 where the crossing is quick already for a relatively large G . (e) We assumed the white noise in Eq. (6) to characterize thermal fluctuations. The underlying assumption is that there is a length scale separation between the long length scale physics of the order parameter dynamics and the presumably short length scale physics of the microscopic degrees of freedom that are integrated out to obtain the order parameter theory. If the microscopic degrees of freedom have a length scale comparable to order parameter length scales, then the partial differential equations we analyse should be replaced by integro-differential equations. Analysis of this situation is beyond the scope of our paper, but we believe that it would not change our main conclusions.

Our work defines directions for future research. On the theoretical side, detailed application of our theory to specific materials, extension to the case of conserved order parameters, to strongly interacting field theories ($G \sim 1$) and to the case of interfaces between domains with different orders

[57] are all of interest. Similar conclusions are expected for quenching through a quantum critical point at zero temperature. Instead of thermal fluctuations, quantum fluctuations will be exponentially amplified. Also, generalization of our formalism to the case where the pump couples coherently to the order parameters, as would happen for Terahertz pumps is of interest. On the experimental side, the growing fluctuations and the induced domain structure (Fig. 1(b)) or the topological vortices can be ideally probed by time-space resolved techniques, e.g., ultra fast Terahertz near field microscopy or ultra fast scanning tunneling microscopy. Moreover, the growing SC fluctuation and thus superfluid density indicates increasing Drude weight in the non equilibrium optical conductivity, leading to novel effects on the collective modes [58] and THz reflectivity.

ACKNOWLEDGMENTS

We acknowledge support from the Department of Energy under Grant DE-SC0018218. We thank M. M. Fogler, R. D. Averitt, D. N. Basov, M. Eckstein, W. Yang, D. Golez and Y. He for helpful discussions.

Note added.—A very recent paper [59] uses similar methods to study the post quench growth of order parameter phase fluctuations.

-
- [1] P. C. Hohenberg and B. I. Halperin, *Rev. Mod. Phys.* **49**, 435 (1977).
 - [2] A. Polkovnikov, K. Sengupta, A. Silva, and M. Vengalattore, *Rev. Mod. Phys.* **83**, 863 (2011).
 - [3] A. J. Bray, *Advances in Physics* **43**, 357 (1994).
 - [4] T. W. B. Kibble, *J. Phys. A* **9**, 1387 (1976).
 - [5] J. S. Langer, M. Bar-on, and H. D. Miller, *Phys. Rev. A* **11**, 1417 (1975).
 - [6] K. Binder, *Reports Prog. Phys.* **50**, 783 (1987).
 - [7] W. C. Carter and W. C. Johnson, eds., *The Selected Works of John W. Cahn* (John Wiley & Sons, Inc., Hoboken, NJ, USA, 1998).
 - [8] R. Alert, P. Tierno, and J. Casademunt, *Nature Communications* **7**, 13067 (2016).
 - [9] W. H. Zurek, *Phys. Rep.* **276**, 177 (1996), 9607135.
 - [10] W. H. Zurek, *Nature* **317**, 505 (1985).
 - [11] G. Biroli, L. F. Cugliandolo, and A. Sicilia, *Phys. Rev. E* **81**, 050101 (2010).
 - [12] A. Chandran, A. Erez, S. S. Gubser, and S. L. Sondhi, *Phys. Rev. B* **86**, 064304 (2012).
 - [13] G. Grüner, *Rev. Mod. Phys.* **60**, 1129 (1988).
 - [14] E. Fradkin, S. A. Kivelson, and J. M. Tranquada, *Rev. Mod. Phys.* **87**, 457 (2015).
 - [15] Y. Tokura, *Reports on Progress in Physics* **69**, 797 (2006).
 - [16] J. Zhang, X. Tan, M. Liu, S. W. Teitelbaum, K. W. Post, F. Jin, K. A. Nelson, D. N. Basov, W. Wu, and R. D. Averitt, *Nat. Mater.* **15**, 956 (2016).
 - [17] D. N. Basov, R. D. Averitt, D. van der Marel, M. Dressel, and K. Haule, *Rev. Mod. Phys.* **83**, 471 (2011).
 - [18] D. Fausti, R. I. Tobey, N. Dean, S. Kaiser, A. Dienst, M. C. Hoffmann, S. Pyon, T. Takayama, H. Takagi, and A. Cavalleri, *Science* **331**, 189 (2011).
 - [19] D. Nicoletti, E. Casandruc, Y. Laplace, V. Khanna, C. R. Hunt, S. Kaiser, S. S. Dhesi, G. D. Gu, J. P. Hill, and A. Cavalleri, *Phys. Rev. B* **90**, 100503(R) (2014).
 - [20] S. J. Zhang, Z. X. Wang, D. Wu, Q. M. Liu, L. Y. Shi, T. Lin, S. L. Li, P. C. Dai, T. Dong, and N. L. Wang, *Phys. Rev. B* **98**, 224507 (2018).
 - [21] S. J. Zhang, Z. X. Wang, L. Y. Shi, T. Lin, M. Y. Zhang, G. D. Gu, T. Dong, and N. L. Wang, *Phys. Rev. B* **98**, 020506(R) (2018).
 - [22] D. Nicoletti, D. Fu, O. Mehio, S. Moore, A. S. Disa, G. D. Gu, and A. Cavalleri, *Phys. Rev. Lett.* **121**, 267003 (2018).
 - [23] K. A. Cremin, J. Zhang, C. C. Homes, G. D. Gu, Z. Sun, M. M. Fogler, A. J. Millis, D. N. Basov, and R. D. Averitt, *Proceedings of the National Academy of Sciences* **116**, 19875 (2019).
 - [24] H. Niwa, N. Yoshikawa, K. Tomari, R. Matsunaga, D. Song, H. Eisaki, and R. Shimano, *Phys. Rev. B* **100**, 104507 (2019).
 - [25] A. Zong, A. Kogar, Y. Q. Bie, T. Rohwer, C. Lee, E. Baldini, E. Ergeçen, M. B. Yilmaz, B. Freelon, E. J. Sie, H. Zhou, J. Straquadine, P. Walmsley, P. E. Dolgirev, A. V. Rozhkov, I. R. Fisher, P. Jarillo-Herrero, B. V. Fine, and N. Gedik, *Nat. Phys.* **15**, 27 (2019).
 - [26] T. Suzuki, T. Someya, T. Hashimoto, S. Michimae, M. Watanabe, M. Fujisawa, T. Kanai, N. Ishii, J. Itatani, S. Kasahara, Y. Matsuda, T. Shibauchi, K. Okazaki, and S. Shin, *Commun. Phys.* **2** (2019), 10.1038/s42005-019-0219-4.
 - [27] M. Rini, R. Tobey, N. Dean, J. Itatani, Y. Tomioka, Y. Tokura, R. W. Schoenlein, and A. Cavalleri, *Nature* **449**, 72 (2007).
 - [28] K. Binder and D. Stauffer, *Adv. Phys.* **25**, 343 (1976).
 - [29] Y. Lemonik and A. Mitra, *Phys. Rev. B* **96**, 104506 (2017).
 - [30] Y. F. Kung, W.-S. Lee, C.-C. Chen, A. F. Kemper, A. P. Sorini,

- B. Moritz, and T. P. Devereaux, *Phys. Rev. B* **88**, 125114 (2013).
- [31] M. Ross Tagaras, J. Weng, and R. E. Allen, *The European Physical Journal Special Topics* (2019), 10.1140/epjst/e2018-800102-6.
- [32] P. E. Dolgirev, A. V. Rozhkov, A. Zong, A. Kogar, N. Gedik, and B. V. Fine, *Phys. Rev. B* **101**, 054203 (2020).
- [33] L. P. Gor'kov and G. M. Eliashberg, *Sov. Phys. JETP* **27**, 328 (1968).
- [34] M. Cyrot, *Reports Prog. Phys.* **36**, 103 (1973).
- [35] H. Kramers, *Physica* **7**, 284 (1940).
- [36] H. Risken, *The Fokker-Planck equation: methods of solution and applications* (Springer-Verlag, Berlin, 1996).
- [37] Z. He and A. J. Millis, *Phys. Rev. B* **93**, 115126 (2016).
- [38] A. Rothwarf and B. N. Taylor, *Phys. Rev. Lett.* **19**, 27 (1967).
- [39] Y. Lemonik and A. Mitra, *Phys. Rev. B* **98**, 214514 (2018).
- [40] A. Kogar, A. Zong, P. E. Dolgirev, X. Shen, J. Straquadine, Y.-Q. Bie, X. Wang, T. Rohwer, I.-C. Tung, Y. Yang, R. Li, J. Yang, S. Weathersby, S. Park, M. E. Kozina, E. J. Sie, H. Wen, P. Jarillo-Herrero, I. R. Fisher, X. Wang, and N. Gedik, *Nature Physics* **16**, 159 (2020).
- [41] D. M. Kennes, E. Y. Wilner, D. R. Reichman, and A. J. Millis, *Nat. Phys.* **13**, 479 (2017).
- [42] M. Babadi, M. Knap, I. Martin, G. Refael, and E. Demler, *Phys. Rev. B* **96**, 014512 (2017).
- [43] M. A. Sentef, A. Tokuno, A. Georges, and C. Kollath, *Phys. Rev. Lett.* **118**, 087002 (2017).
- [44] G. Chiriacò, A. J. Millis, and I. L. Aleiner, *Phys. Rev. B* **98**, 220510(R) (2018).
- [45] Y. Wang, C.-C. Chen, B. Moritz, and T. P. Devereaux, *Phys. Rev. Lett.* **120**, 246402 (2018).
- [46] C. L. Smallwood, J. P. Hinton, C. Jozwiak, W. Zhang, J. D. Koralek, H. Eisaki, D.-H. Lee, J. Orenstein, and A. Lanzara, *Science* **336**, 1137 (2012).
- [47] F. Giusti, A. Marciniak, F. Randi, G. Sparapassi, F. Boschini, H. Eisaki, M. Greven, A. Damascelli, A. Avella, and D. Fausti, *Phys. Rev. Lett.* **122**, 067002 (2019).
- [48] M. Eichberger, H. Schäfer, M. Krumova, M. Beyer, J. Demsar, H. Berger, G. Moriena, G. Sciaini, and R. J. D. Miller, *Nature* **468**, 799 (2010).
- [49] N. Erasmus, M. Eichberger, K. Haupt, I. Boshoff, G. Kassier, R. Birmurske, H. Berger, J. Demsar, and H. Schwoerer, *Phys. Rev. Lett.* **109**, 167402 (2012).
- [50] J. P. Hinton, J. D. Koralek, Y. M. Lu, A. Vishwanath, J. Orenstein, D. A. Bonn, W. N. Hardy, and R. Liang, *Phys. Rev. B* **88**, 060508(R) (2013).
- [51] B. Michon, C. Girod, S. Badoux, J. Kačmarčík, Q. Ma, M. Dragomir, H. A. Dabkowska, B. D. Gaulin, J. S. Zhou, S. Pyon, T. Takayama, H. Takagi, S. Verret, N. Doiron-Leyraud, C. Marcenat, L. Taillefer, and T. Klein, *Nature* **567**, 218 (2019).
- [52] P. G. Radaelli, D. G. Hinks, A. W. Mitchell, B. A. Hunter, J. L. Wagner, B. Dabrowski, K. G. Vandervoort, H. K. Viswanathan, and J. D. Jorgensen, *Phys. Rev. B* **49**, 4163 (1994).
- [53] F. Zhou, J. Williams, C. D. Malliakas, M. G. Kanatzidis, A. F. Kemper, and C.-Y. Ruan, arXiv e-prints, arXiv:1904.07120 (2019), arXiv:1904.07120 [cond-mat.mes-hall].
- [54] A. S. McLeod, J. Zhang, M. Q. Gu, F. Jin, G. Zhang, K. W. Post, X. G. Zhao, A. J. Millis, W. Wu, J. M. Rondinelli, R. D. Averitt, and D. N. Basov, “Multi-messenger nano-probes of hidden magnetism in a strained manganite,” (2019), arXiv:1910.10361 [cond-mat.mes-hall].
- [55] E. Guardado-Sanchez, P. T. Brown, D. Mitra, T. Devakul, D. A. Huse, P. Schauf, and W. S. Bakr, *Phys. Rev. X* **8**, 021069 (2018).
- [56] C. R. Hunt, D. Nicoletti, S. Kaiser, T. Takayama, H. Takagi, and A. Cavalleri, *Phys. Rev. B* **91**, 020505 (2015).
- [57] L. Del Re, M. Fabrizio, and E. Tosatti, *Phys. Rev. B* **93**, 125131 (2016).
- [58] Z. Sun, D. N. Basov, and M. M. Fogler, *Phys. Rev. Lett.* **117**, 076805 (2016).
- [59] P. E. Dolgirev, M. H. Michael, A. Zong, N. Gedik, and E. Demler, “Universal dynamics of order parameter fluctuations in pump-probe experiments,” (2019), arXiv:1910.02518 [cond-mat.other].
- [60] R. Landauer and J. A. Swanson, *Phys. Rev.* **121**, 1668 (1961).

Appendix A: Equilibrium Free Energy and Phase Diagram

1. Competing orders

The phase diagram is shown in Fig. 8. We write Eq. (2) for the spatially uniform case using Eq. (3) and writing $\psi_1^2 = R^2 \cos^2 \theta$, $\psi_2 = R^2 \sin^2 \theta$. We obtain

$$f = -\frac{\alpha_1 + \alpha_2}{2} R^2 - \frac{\alpha_1 - \alpha_2}{2} R^2 \cos 2\theta + R^4 \frac{1 + \frac{c}{2}}{2} + R^4 \frac{1 - \frac{c}{2}}{2} \cos^2 2\theta \quad (\text{A1})$$

Minimizing with respect to $\cos 2\theta$ gives

$$\cos 2\theta = \frac{\alpha_1 - \alpha_2}{2R^2(2 - c)} \quad (\text{A2})$$

so

$$f = -\frac{\alpha_1 + \alpha_2}{2} R^2 - \frac{(\alpha_1 - \alpha_2)^2}{8(1 - \frac{c}{2})} + R^4 \frac{1 + \frac{c}{2}}{2} \quad (\text{A3})$$

and minimizing over R gives

$$R^2 = \frac{\alpha_1 + \alpha_2}{2 + c} \quad (\text{A4})$$

so

$$f = -\frac{(\alpha_1 + \alpha_2)^2}{4(2+c)} - \frac{(\alpha_1 - \alpha_2)^2}{8(1-\frac{c}{2})} \quad (\text{A5})$$

and

$$\cos 2\theta = \frac{\alpha_1 - \alpha_2}{2(\alpha_1 + \alpha_2)} \frac{2+c}{2-c} \quad (\text{A6})$$

The alternative solution is to set one of the $\psi = 0$, obtaining

$$f = -\frac{\alpha_i^2}{2} \quad (\text{A7})$$

Thus we see that if $c > 2$ then the mixed solution costs energy and lower energy solutions are $2\theta = 0$ and π . Expanding around the $\theta = 0$ solution we obtain

$$f(\theta) - f(\theta = 0) = \frac{\alpha_1^2 - \alpha_1\alpha_2}{4}\theta^2 - \frac{\alpha_1^2}{8}\left(1 - \frac{c}{2}\right)2\theta^2 + \mathcal{O}\theta^4 \quad (\text{A8})$$

or

$$f(\theta) - f(\theta = 0) = \frac{\alpha_1^2}{4}\left(\frac{c}{2} - \frac{\alpha_1}{\alpha_2}\right)\theta^2 + \mathcal{O}\theta^4 \quad (\text{A9})$$

so we see that the minimum at $\psi_2 = 0$ is only stable if $\frac{c}{2} > \frac{\alpha_1}{\alpha_2}$; expanding around the other minimum changes the sign of the θ^2 term and interchanges α_2 and α_1 , justifying the inequalities presented in the main text.

2. Intertwined orders

We write Eq. (2) for the spatially uniform case using Eq. (3) and Eq. (47), now in their original form

$$f = -\alpha_1\psi_1^2 - \alpha_2\psi_2^2 + \psi_1^4 + \psi_2^4 + c\psi_1^2\psi_2^2 + d_1\psi_1^4\psi_2^2 \quad (\text{A10})$$

We suppose $0 < c < 2$ and $d_1 > 0$, assume $T_{c2} > T > T_{c1}$ and consider the physics as T is decreased below T_{c2} . Initially we have a solution with $\psi_2^2 = \frac{\alpha_2}{2}$ and $\psi_1 = 0$. As the temperature is decreased, $\alpha_1 - c\alpha_2/2$ may become positive; if this occurs, a ψ_1 component is added to the solution with $\psi_2 \neq 0$. This instability takes place at a temperature lower than T_{c1} if $c > 0$ and at a temperature higher than T_{c1} if $c < 0$. We interpret this mixed state as having intertwined order, since both order parameters are non-zero. As T is decreased below T_{c1} a second extremum (saddle point) appears at $\psi_1^2 = \frac{\alpha_1}{2}$, $\psi_2 = 0$. After α_1 becomes large enough such that $\frac{c|\alpha_1|}{2} + d\frac{\alpha_1^2}{4} > \alpha_2$, this saddle point becomes stable to variations in ψ_2 and thus a local minimum.

Appendix B: The Fokker-Planck Equation and its Approximations

If one defines the probability functional $\rho[\psi]$, the stochastic TDGL equation (1) is equivalent to the Fokker-Planck equation [1] for the probability functional $\rho[\psi(\mathbf{r}, t)]$:

$$\partial_t \rho = \frac{1}{E_c} \sum_i \int d^D \mathbf{r} \gamma_i \partial_{\psi_i} (\rho \partial_{\psi_i} F + T \partial_{\psi_i} \rho). \quad (\text{B1})$$

where ∂_{ψ_i} should be understood as functional derivative: $\partial_{\psi_i} \equiv \frac{\partial}{\partial \psi_i(\mathbf{r}, t)}$. The averages $\langle \psi^2 \rangle$ taken throughout the paper is over the probability functional $\rho[\psi(\mathbf{r}, t)]$. The order parameter can be written as a uniform field plus small fluctuations:

$$\psi_i(\mathbf{r}, t) = \bar{\psi}_i(t) + \delta\psi_i(\mathbf{r}, t) = \bar{\psi}_i(t) + \sum_{k \neq 0} \psi_i(k) e^{i\mathbf{k}\mathbf{r}}. \quad (\text{B2})$$

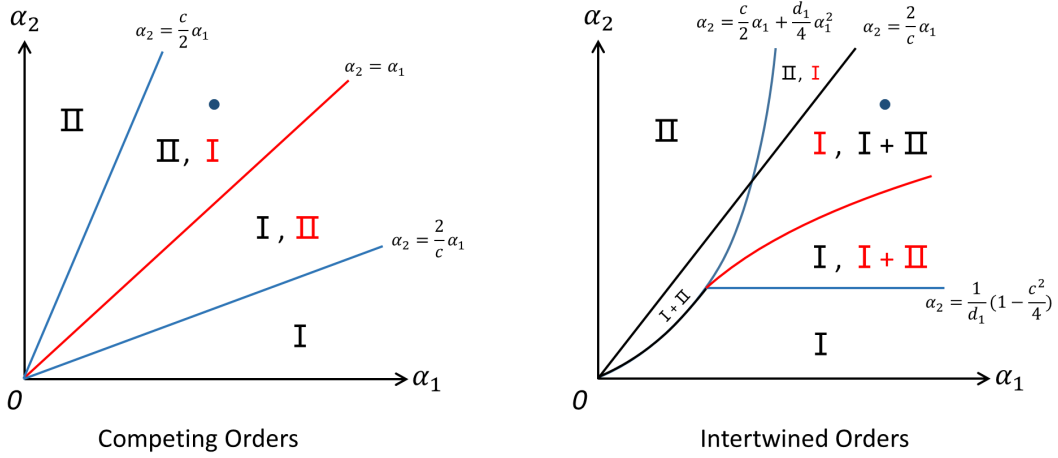


FIG. 8. Equilibrium phase diagrams on the α_1 v.s. α_2 plane. Black roman numeral indicates the corresponding phase is a global minimum. Red one indicates local minimum. $I+II$ means a minimum with both orders nonzero. The competing orders case corresponds to $c > 2$ and $d_1 = 0$. The intertwined orders case corresponds to $0 < c < 2$ and $d_1 > 0$. The systems are assumed to be at the blue dots in equilibrium.

Our mean field plus fluctuation theory can be viewed as an expansion in terms of the Ginzburg parameter G , or equivalently, the small noise term $\eta(\mathbf{r}, t)$. The uniform background is the zeroth order term in the random noise $\eta(\mathbf{r}, t)$. The TDGL equation thus leads to the coupled equations of the uniform background and the fluctuations

$$\begin{aligned} \frac{1}{\gamma_i} \partial_t \bar{\psi}_i(t) &= \left(-\frac{\delta F}{\delta \psi_i(\mathbf{r}, t)} + \eta_i(\mathbf{r}, t) \right)_0 = -\partial_{\bar{\psi}_i} F + \eta_{i0}(t) + O(\eta^2), \\ \frac{1}{\gamma_i} \partial_t \psi_i(k, t) &= \left(-\frac{\delta F}{\delta \psi_i(\mathbf{r}, t)} + \eta_i(\mathbf{r}, t) \right)_k = 2\alpha_{ik} \psi_i(k) - \left(4\psi_i^3 + 2c\psi_i\psi_j^2 + O(\psi^5) \right)_k + \eta_{ik}(t) \end{aligned} \quad (B3)$$

where $\langle \rangle_k$ mean the Fourier component with momentum k , $\eta_{ik}(t)$ means the k momentum component of the noise, $j \neq i$ represents the other order different from order i . Multiplying the second equation by $\psi_{-k}(t)$ and taking the average over the probability functional ρ , one obtains the equation of motion for the second moment:

$$\frac{1}{\gamma_i} \partial_t \langle \psi_i(k) \psi_i(-k) \rangle = 4\alpha_{ik} \langle \psi_i(k) \psi_i(-k) \rangle - 2 \left\langle \psi_{i,-k} \left(4\psi_i^3 + 2c\psi_i\psi_j^2 + O(\psi^5) \right)_k \right\rangle + 2 \langle \psi_i(-k) \eta_{ik}(t) \rangle. \quad (B4)$$

If one keeps only $O(\eta^2)$ terms, the equation for the second moment $\langle \psi_i(k) \psi_j(-k) \rangle$ simplifies to

$$\partial_t \langle \psi_i(k) \psi_j(-k) \rangle = - \left(\partial_{\bar{\psi}_\mu} \partial_{\bar{\psi}_\nu} F + 2\xi_{\mu\nu}^2 k^2 \right) (\gamma_{i\nu} \langle \psi_\mu(k) \psi_j(-k) \rangle + \gamma_{j\nu} \langle \psi_\mu(k) \psi_i(-k) \rangle) + 2T_v \gamma_{ij} \quad (B5)$$

where

$$\xi_{\mu\nu} = \begin{pmatrix} \xi_{10} & 0 \\ 0 & \xi_{20} \end{pmatrix}, \quad \gamma_{\mu\nu} = \begin{pmatrix} \gamma_1 & 0 \\ 0 & \gamma_2 \end{pmatrix} \quad (B6)$$

and repeated indices should be summed over. Note that $T_v = T/(E_c V)$ is the temperature normalized to the condensation energy of the whole volume. Therefore, the fluctuation just evolves in a time dependent quadratic potential determined by the curvature of the local free energy landscape taken at $\bar{\psi}(t)$. In principle, one could make a ‘mean field’ approximation by assuming the probability function ρ is always a Gaussian function and easily take into account the fluctuation correction to Eq. (B5). But this is out of the scope of this paper.

The linearized Fokker-Plank equation close to point O reads

$$\partial_t \rho = \partial_{\psi(k)} \left(-2\gamma \alpha_k(t) \psi(k) \rho + \gamma T_v(t) \partial_{\psi(k)} \rho \right). \quad (B7)$$

where α and T_v are time dependent and $\alpha_k(t) = \alpha(t) - \xi_0^2 k^2$. This is a diffusion equation for the probability $\rho(\psi_k)$ in the quadratic potential $-\alpha_k \psi(k)^2$ with diffusion constant γT_v . The exact solution to Eq. (B7) is the Gaussian function Eq. (5) with the variance satisfying (here and below we denote $\psi(k)$ as ψ_k for simplicity)

$$\partial_t \langle \psi_k^2 \rangle = 4\gamma \alpha_k(t) \langle \psi_k^2 \rangle + 2T_v(t) \gamma. \quad (B8)$$

The solution to Eq. (B8) is

$$\langle \psi_k^2 \rangle_t = \langle \psi_k^2 \rangle_{t'} e^{2S_k(t, t')} + 2\gamma \int_{t'}^t dt'' T_v(t'') e^{2S_k(t, t'')} \quad (\text{B9})$$

which could be obtained by squaring

$$\psi_k(t) = \int_0^t dt' G_k(t, t') \eta_k(t') + \psi_k(0) e^{S_k(t)} \quad (\text{B10})$$

where $G_k(t, t') = \Theta(t - t') e^{S_k(t, t')}$ is the Green's function for Eq. (8) of the main text and $S_k(t, t') = 2\gamma \int_{t'}^t dx \alpha_k(x)$ is the accumulated exponent.

Appendix C: Dynamics

We evaluate Eq. (29) of the main text, which together with the initial condition term is

$$D_k(t) \equiv \langle \psi_k(t) \psi_{-k}(t) \rangle = D_k(-t_{\text{pump}}) e^{2S_k(t, -t_{\text{pump}})} + 2\gamma \int_{-t_{\text{pump}}}^t dt' e^{2S_k(t, t')} T(t') \quad (\text{C1})$$

where the accumulated exponent is

$$S_k(t, t') = 2\gamma \int_{t'}^t dt'' (\alpha(t'') - \xi_0^2 k^2) \quad (\text{C2})$$

and T should be understood as the dimensionless quantity $T/(E_c V)$ here and in the following. The integral in Eq. (12) describes the contributions to the variance $D_k(t)$ from noise fluctuations that are created at time t' and then propagated forward by the equation of motion. The pump and cooling profile determines the time dependence of D_k and the needed expressions may be straightforwardly evaluated for any pump and cooling profile. Within the linear cooling profile approximation of Figure 2, S_k and T are combinations of quadratic, linear and constant functions of time and analytic results can be written down in terms of error functions, Gaussians and exponentials. We present here further analytical work based on the linear cooling profile that brings insight.

At times $t < t_0$, $S_k < 0$ for all k so fluctuations created at a time $t < t_0$ decay as time increases to t_0 . At times $t > t_0$ long wavelength fluctuations ($k^2 \xi_0^2 < \alpha(t)$) increase exponentially with time. Thus t_0 is a convenient reference point and we are interested in times t greater than t_0 . Separating the integral into times greater and less than t_0 and noting that $S(t, t') = S(t, t_0) + S(t_0, t')$ and that $S(t, t') = -S(t', t)$ we have

$$D_k(t) = e^{2S_k(t, t_0)} \left(D_k^{(1)} + D_k^{(2)}(t) \right) \quad (\text{C3})$$

with

$$D_k^{(1)} = D_k(-t_{\text{pump}}) e^{2S_k(t_0, -t_{\text{pump}})} + 2\gamma \int_{-t_{\text{pump}}}^{t_0} dt' e^{2S_k(t_0, t')} T(t') \quad (\text{C4})$$

and

$$D_k^{(2)}(t) = 2\gamma \int_{t_0}^t dt' e^{-2S_k(t', t_0)} T(t'). \quad (\text{C5})$$

The first term ($D^{(1)}$) describes the contribution to the variance of fluctuations created before t_0 and propagated forward to t and the second term ($D^{(2)}$), which we have rearranged for later convenience, describes the additional contributions of fluctuations occurring after t_0 . We are interested in the case in which the fluctuations at $t = t_0$ are very small, and we wish to focus on long times such that the growing modes have increased to an amplitude of the order of unity. In this circumstance a general asymptotic analysis is possible but for ease of writing we will focus on the linear cooling profile for which

$$T(t) = \begin{cases} T_H & (-t_{\text{pump}} < t < 0) \\ T_H \left(1 - \frac{t}{t_0}\right) + T_C \frac{t}{t_0} & (0 < t < t_0) \\ T_C \frac{t_m - t}{t_m - t_0} + T_L \frac{t - t_0}{t_m - t_0} & (t_0 < t < t_m) \\ T_L & (t > t_m) \end{cases} \quad (\text{C6})$$

and

$$\alpha(t) = \begin{cases} \alpha_H & (-t_{\text{pump}} < t < 0) \\ \alpha_H \left(1 - \frac{t}{t_0}\right) & (0 < t < t_0) \\ \alpha_L \frac{t-t_0}{t_m-t_0} & (t_0 < t < t_m) \\ \alpha_L & (t > t_m) \end{cases}. \quad (\text{C7})$$

We begin with $D^{(1)}$ which we rewrite as

$$D_k^{(1)} = D_H + D_{KZ} \quad (\text{C8})$$

where D_H describes the propagation forward in time of the fluctuations existing before the pump was turned on and created by the pump. Using the linear cooling profile formulas and the definition of S

$$D_H = e^{-2\gamma t_0(|\alpha_H| + 2\xi_0^2 k^2)} \left(\frac{T_H \left(1 - e^{-4\gamma t_{\text{pump}}(|\alpha_H| + \xi_0^2 k^2)}\right)}{2(|\alpha_H| + \xi_0^2 k^2)} + \frac{T_L e^{-4\gamma t_{\text{pump}}(|\alpha_H| + \xi_0^2 k^2)}}{2(2\alpha_L + \xi_0^2 k^2)} \right) \quad (\text{C9})$$

The requirement that the mean field order parameter be completely suppressed means that $e^{-2|\alpha_H|(2t_{\text{pump}} + t_0)} \ll G/\alpha_L$ so

$$D_H \approx \frac{T_H}{2(|\alpha_H| + \xi_0^2 k^2)} e^{-2\gamma t_0(|\alpha_H| + 2\xi_0^2 k^2)} \quad (\text{C10})$$

which represents the hot thermal fluctuations created by the pump propagated to $t = t_0$.

We now turn to D_{KZ} which represents the fluctuations created as the system cools from $t = 0$ to $t = t_0$ after the pump is turned off:

$$D_{KZ} = 2\gamma \int_0^{t_0} dt' e^{2S_k(t_0, t')} T(t') \quad (\text{C11})$$

$$= 2\gamma t_0 \int_0^1 du e^{-2\gamma t_0|\alpha_H|u^2 - 4\gamma t_0 k^2 \xi_0^2 u} (T_H u + T_c(1-u)) \quad (\text{C12})$$

where in the second equality we have defined $u = (t_0 - t)/t_0$. In the rapid cooling limit $|\alpha_H|\gamma t_0 \ll 1$ D_{KZ} is $\mathcal{O}(\gamma t_0)$ and is much smaller than D_H . In the slow cooling limit the integral is dominated by small u , and we may extend the upper limit to infinity and rescale $u = v/(\sqrt{2}|\alpha_H|\gamma t_0)$ obtaining

$$D_{KZ} = \frac{T_c}{\alpha_{KZ}} \int_0^\infty dv e^{-v^2 - 2k^2 \xi_{KZ}^2 v} \quad (\text{C13})$$

where we have defined the important length and time scales

$$\alpha_{KZ} = \sqrt{\frac{|\alpha_H|}{2\gamma t_0}} = \sqrt{\frac{|\alpha_H| + \alpha_L}{2\gamma t_m}}; \quad \xi_{KZ}^2 = \xi_0^2 / \alpha_{KZ}; \quad t_{KZ} = \sqrt{\frac{t_m}{2\gamma(|\alpha_H| + \alpha_L)}}. \quad (\text{C14})$$

We see that for $k^2 \xi_{KZ}^2 \ll 1$, $D_{KZ} \approx \frac{T_c}{2\alpha_{KZ}} \sqrt{\pi}$ and for $k^2 \xi_{KZ}^2 \gg 1$, $D_{KZ} \sim \frac{T_c}{2k^2 \xi_0^2}$. This is the expected behavior of a critical theory with mean field exponents and an effective distance from criticality determined by the cooling rate, consistent with the general analysis of Kibble and Zurek [4, 9, 10].

We now present a qualitative evaluation of $D^{(2)}(t)$. We have $S_k(t, t_0) = S_0(t, t_0) - 2\xi_0^2 k^2(t - t_0)$ with

$$S_0(t, t_0) = \alpha_L \frac{(t - t_0)^2}{t_m - t_0} \Theta(t_m - t) + 2\alpha_L \left(t - \frac{t_m + t_0}{2}\right) \Theta(t - t_m). \quad (\text{C15})$$

We are interested in growing modes, for which $\frac{S_0(t, t_0)}{t - t_0} > k^2 \xi_0^2$; roughly these are those for which $\alpha_L > k^2 \xi_0^2$. In the slow cooling case $\alpha_L \gamma (t_m - t_0) = \frac{\alpha_L^2}{|\alpha_H| + \alpha_L} \gamma t_m > 1$. In the fast cooling limit, we may set $t_m - t_0 = 0$ and write

$$D_k^{(2)}(t) = 2\gamma T_L \int_{t_0}^t dt' e^{-4\gamma(t' - t_0)(\alpha_L - \xi_0^2 k^2)} = \frac{T_L}{2(\alpha_L - \xi_0^2 k^2)} \left(1 - e^{-4\gamma(t - t_0)(\alpha_L - \xi_0^2 k^2)}\right) \approx \frac{T_L}{2\gamma \alpha_L} \quad (\text{C16})$$

Here we have neglected k -dependence, which is on a scale that is not relevant at large enough t . In the ultra slow cooling case we have for $t < t_m$ and defining $u = \frac{t' - t_0}{t_m - t_0}$

$$D^{(2)}(t) = 2\gamma(t_m - t_0) \int_0^{u_{max}} du e^{-2\alpha_L \gamma(t_m - t_0) u^2 + 4\gamma(t_m - t_0) u k^2 \xi_0^2} (T_c(1 - u) + T_L u) \quad (C17)$$

with $u_{max} = \frac{t - t_0}{t_m - t_0}$. The argument of the exponential is maximized at $u = u^* = \frac{\xi_0^2 k^2}{\alpha_L}$ (for growing modes $u_{max} > 2\xi_0^2 k^2 / \alpha_L$ so u^* is within integration range). Defining $u = u^* + \frac{v}{2\sqrt{\gamma(t_m - t_0)}}$ and noting that $t_m - t_0 = t_m \frac{\alpha_L}{|\alpha_H| + \alpha_L}$ we have (after integrating over v using saddle point approximation)

$$D_k^{(2)}(t) = \frac{\sqrt{\pi}}{2} e^{\xi_{KZ}^4 k^4} \frac{1}{\alpha_{KZ}} (T_c(1 - u^*) + T_L u^*) \quad (C18)$$

Note that we have kept only half of the Gaussian integral. This is valid for the modes $\xi_0^2 k^2 \lesssim \frac{1}{4\gamma(t - t_0)} \ll \frac{1}{\sqrt{8\gamma(t_m - t_0)/\alpha_L}}$ which are the only relevant ones at long time $t - t_0$. The exponent is also small in this limit so to an adequate approximation we have

$$D^{(2)}(t) = \sqrt{\pi} \frac{T_c}{2\alpha_{KZ}} \quad (C19)$$

which is the same as the $k \rightarrow 0$ limit of $D_k^{(1)} \approx D_{KZ}$. This is expected since $D_k^{(2)}$ can be interpreted as the fluctuations created after t_0 and back propagated to t_0 . This is symmetric to $D_k^{(1)}$ for $k \rightarrow 0$ in the slow cooling limit.

Appendix D: Exact solution in terms of error functions

The $D_k^{(1)} = D_H + D_{KZ}$ in Eq. (C3) has the interpretation of the fluctuation prepared at time t_0 . The exact form of D_H is Eq. (C9). In the linear cooling profile approximation used in this paper, the exact form of D_{KZ} is

$$D_{KZ} = \frac{T_c}{2\alpha_{KZ}} \left[\sqrt{\pi} \left(1 - \left(\frac{T_H}{T_c} - 1 \right) \frac{\xi_{KZ}^2 k^2}{\alpha_H} \right) e^{\xi_{KZ}^4 k^4} \text{Erf} \left[\xi_{KZ}^2 k^2, \xi_{KZ}^2 k^2 + \sqrt{2\gamma|\alpha_H|} t_0 \right] - \left(\frac{T_H}{T_c} - 1 \right) \frac{t_{KZ}}{t_0} (e^{2S_k(t_0, 0)} - 1) \right] \quad (D1)$$

where $\text{Erf}[x_1, x_2] = \frac{2}{\sqrt{\pi}} \int_{x_1}^{x_2} e^{-x^2} dx$ is the error function.

For the $D_k^{(2)}$ term, it is simpler to neglect the time dependence of the noise, i.e., take $T_c = T_L$, after which one obtains

$$D_k^{(2)}(t) = \begin{cases} g_k(t_m, t), & t < t_m \\ g_k(t_m, t_m) + \frac{T_L}{2(\alpha_L - \xi_0^2 k^2)} e^{-2S_k(t_m, t_0)} (1 - e^{-2S_k(t, t_m)}), & t \geq t_m \end{cases} \quad (D2)$$

where we have defined

$$g_k(t_m, t) = \sqrt{\pi} \frac{T_L}{2\alpha_{KZ}} e^{\xi_{KZ}^4 k^4} \text{Erf} \left[-\xi_{KZ}^2 k^2, -\xi_{KZ}^2 k^2 + t/t_{KZ} \right]. \quad (D3)$$

One can take various limits of Eq. (D1) and (D2) to get the results in the previous section.

Appendix E: The fast cooling limit: $t_m = 0$

For $t_m = 0$ and neglecting the initial condition at $t = t_{pump}$, Eq. (12) reduces to

$$D_k = \frac{1}{2} \left(\frac{T_L}{\alpha_L - \xi_0^2 k^2} + \frac{T_H}{|\alpha_H| + \xi_0^2 k^2} \right) e^{4\gamma t(\alpha_L - \xi_0^2 k^2)} - \frac{1}{2} \frac{T_L}{\alpha_L - \xi_0^2 k^2}. \quad (E1)$$

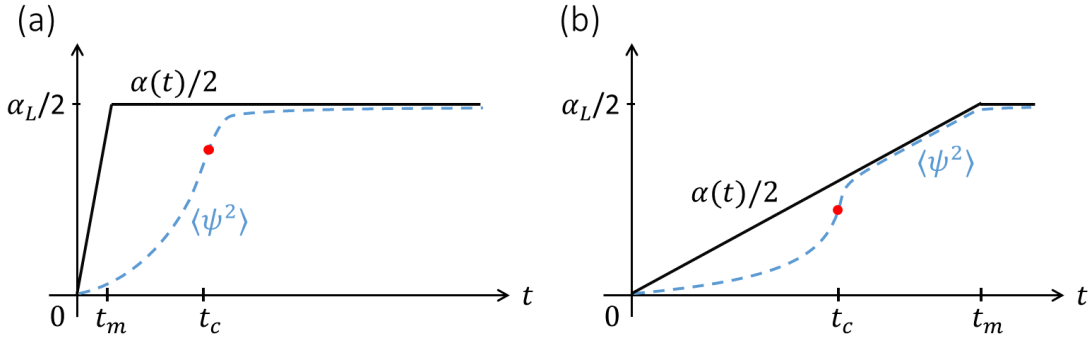


FIG. 9. Illustration of the evolution of order parameter fluctuation in (a) the fast cooling case and (b) the slow cooling case.

Summing up contribution from all the Fourier modes, one obtains the real space correlation function

$$\langle \psi(0)\psi(r) \rangle = V(2\pi)^{-D} \int d^D \mathbf{k} e^{i\mathbf{k}\mathbf{r}} \langle \psi_k^2 \rangle. \quad (\text{E2})$$

At long time $4\gamma\alpha_L t \gg 1$, D_k is approximately a gaussian function in k and the Fourier transform becomes

$$\begin{aligned} \langle \psi(0)\psi(r) \rangle &\approx \left(\frac{G(T_L)}{2\alpha_L} + \frac{G(T_H)}{2|\alpha_H|} \right) \left(\frac{1}{16\pi\gamma t} \right)^{D/2} e^{4\alpha_L\gamma t} e^{-r^2/(2\xi(t)^2)} \\ &= \frac{\alpha_L}{2} \left(\left(1 + \frac{G(T_H)\alpha_L}{G(T_L)|\alpha_H|} \right) (4\pi)^{-D/2} \alpha_L^{D/2-2} G(T_L) \right) \left(\frac{1}{4\alpha_L\gamma t} \right)^{D/2} e^{4\alpha_L\gamma t} e^{-r^2/(2\xi(t)^2)} \\ &= \frac{\alpha_L}{2} \zeta \left(\frac{1}{4\alpha_L\gamma t} \right)^{D/2} e^{4\alpha_L\gamma t} e^{-r^2/(2\xi(t)^2)} \end{aligned} \quad (\text{E3})$$

where $\xi(t) = \xi_0 \sqrt{8\gamma t}$ is the universal correlation growth law and

$$\zeta = \left(1 + \frac{G(T_H)\alpha_L}{G(T_L)|\alpha_H|} \right) (4\pi)^{-D/2} \alpha_L^{D/2-2} G(T_L) \sim 2(4\pi)^{-D/2} \alpha_L^{D/2-2} G(T_L) \quad (\text{E4})$$

is the Ginzburg parameter for critical phenomenon at equilibrium. Thus the fluctuation $\langle \psi_i(0)^2 \rangle$ grows exponentially with time and ψ_1 grows faster due to a larger $\alpha_{1L}\gamma_1$. Setting $\langle \psi(0)^2 \rangle = \alpha_L/2$ gives the crossover time

$$4\alpha_L\gamma t_c = \ln \frac{1}{\zeta} + \frac{D}{2} \ln(4\alpha_L\gamma t_c). \quad (\text{E5})$$

At this time, keeping the first two terms in the \ln expansion of t_c , the ratio between the fluctuations in the two directions is

$$\frac{\langle \psi_2^2 \rangle}{\langle \psi_1^2 \rangle} \approx \frac{\alpha_{1L}}{\alpha_{2L}} \frac{G_2}{G_1} \left(\frac{\gamma_1}{\gamma_2} \right)^{D/2} \left(\frac{1}{\zeta_1} \left(\ln \frac{1}{\zeta_1} \right)^{D/2} \right)^{\frac{\alpha_{2L}\gamma_2}{\alpha_{1L}\gamma_1} - 1}. \quad (\text{E6})$$

Appendix F: The slow cooling case in competing order systems

The slow cooling case is characterized by a large t_m . After t_1 , ψ_1 starts to grow exponentially while ψ_2 has been growing for a time of $t_1 - t_2$. Assume both order parameters are in the exponential growing stage and nonlinearity is not yet on set, they obey the equation

$$\langle \psi_i(0)\psi_i(r) \rangle_t = \frac{\sqrt{\pi} G_i / \alpha_{iKZ}}{(16\pi\gamma_i(t-t_i))^{\frac{D}{2}}} e^{2\gamma_i(\alpha_{iL} + |\alpha_{iH}|)(t-t_i)/t_m} e^{-\frac{r^2}{2\xi_i(t)^2}}. \quad (\text{F1})$$

The crossover of ψ_i to nonlinearity happens at $\langle \psi_i(0)^2 \rangle_t = \alpha_i(t)$ which yields

$$1 = \zeta_i x_i^{-\frac{D}{4}-1/2} e^{x_i}, \quad x_i = \ln \frac{1}{\zeta_{mi}} + \frac{D}{4} \ln x_i, \quad (\text{F2})$$

where $x_i = 2\gamma_i(\alpha_{iL} + |\alpha_{iH}|)(t - t_i)^2/t_m$ and

$$\zeta_{mi} = 2^{-7D/4+1}\pi^{1/2-D/2}\left(\frac{\gamma_i t_m}{\alpha_{iL} + |\alpha_{iH}|}\right)^{-D/4+1} G_i = 2^{-3D/4}\pi^{1/2}\left(\frac{\alpha_L^2 \gamma_i t_m}{\alpha_{iL} + |\alpha_{iH}|}\right)^{-D/4+1} \zeta_i \sim \zeta_i. \quad (F3)$$

To leading order in the \ln expansion we have for order I :

$$t_c - t_1 \approx \left(\frac{t_m}{2(\alpha_{1L} + |\alpha_{1H}|)\gamma_1} \ln \frac{1}{\zeta_{m1}}\right)^{1/2}. \quad (F4)$$

At time t_c , the correlation length of the fluctuations is $\xi \approx 2\sqrt{2}\left(\frac{\gamma t_m}{2(\alpha_{1L} + |\alpha_{1H}|)} \ln \frac{1}{\zeta}\right)^{1/4} \xi_0 \sim (\gamma t_m \ln \frac{1}{\zeta})^{1/4} \xi_0$, which predicts a logarithmic correction to the $\xi \sim t_m^{1/4}$ Kibble-Zurek scaling [10]. Note that the logarithmic correction could be numerically large for very small ζ . In 2D, the number density of topological vortices created is thus $n \sim 1/\xi(t_c)^2 \sim (\gamma t_m \ln \frac{1}{\zeta})^{-1/2} \xi_0^{-2}$. For the mean field plus fluctuation theory to be valid, we also require $G\alpha(t)^{D/2-2} \ll 1$ at the predicted t_c for $D < 4$, in other words:

$$\left(\frac{t_m}{2(\alpha_{1L} + |\alpha_{1H}|)\gamma_1} \ln \frac{1}{\zeta_{m1}}\right)^{1/2} \frac{\alpha_{1L} + |\alpha_{1H}|}{t_m} \gg \left(\frac{1}{G}\right)^{1/(D/2-2)} \quad (F5)$$

which yields

$$t_m \gamma_1 \ll \left(\frac{1}{G}\right)^{-1/(D/4-1)} \frac{\alpha_{1L} + |\alpha_{1H}|}{2} \ln \frac{1}{\zeta_{m1}} \sim \left(\frac{1}{\zeta}\right)^{\frac{1}{1-D/4}}. \quad (F6)$$

Trapping into the metastable minimum requires that $\langle \psi_2(0)^2 \rangle \ll \langle \psi_1(0)^2 \rangle$ at t_m . Simply comparing the exponents yields

$$t_m \ll \frac{\left(\left(\frac{1}{\gamma_2} \frac{1}{a_{2L}-a_{2H}}\right)^{1/2} - \left(\frac{1}{\gamma_1} \frac{1}{a_{1L}-a_{1H}}\right)^{1/2}\right)^2}{2\lambda_d^2} \ln \frac{1}{\zeta_{m1}}. \quad (F7)$$

where $\lambda_d = (t_1 - t_2)/t_m$. This imposes the criterion

$$\Delta \ll \frac{1}{r} \left(\sqrt{\frac{2\lambda_d^2 (\alpha_{1L} + |\alpha_{1H}|)}{\ln \frac{1}{\zeta_{m1}}} \gamma_1 t_m + 1} \right)^{-2} \approx \frac{1}{r} \left(\sqrt{\frac{2\lambda_d^2 (\alpha_{1L} + |\alpha_{1H}|)}{\ln \frac{1}{\zeta_1}} \gamma_1 t_m + 1} \right)^{-2} \equiv f_2(\gamma_1 t_m). \quad (F8)$$

By assuming $\zeta = 10^{-4}$, $\gamma_1 = 2\text{ps}^{-1}$, $(\alpha_{1L}, \alpha_{2L}) = (1, 1.1)$ and $(\alpha_{1H}, \alpha_{2H}) = (-1, -0.9)$, one obtains $t_{mu} \approx 4.6\text{ps}$ and $t_{ms} \approx 460\text{ps}$. Since the typical cooling time due to electron phonon thermalization ranges from 1ps to 100ps, most ultrafast experiments are in the regime analyzed in this paper (Fig. 5).

Appendix G: The pumping process

The pump brings α_{iL} to $\alpha_{iH} < 0$ as shown in Fig. 2 which induces the order parameter dynamics from point II to O in Fig. 1(a). At mean field level, this nonlinear dynamics is described by Eq. (B3) and the uniform component obeys the exact solution

$$\bar{\psi}_2^2(t) = \frac{-\alpha_{2H}/2}{(1 - \alpha_{2H}/\alpha_{2L})e^{-4\alpha_{2H}\gamma_2(t+t_{pump})} - 1}. \quad (G1)$$

The long time asymptotic form is $\bar{\psi}_2^2 = \frac{-\alpha_{2H}/2}{(1 - \alpha_{2H}/\alpha_{2L})} e^{4\alpha_{2H}\gamma_2(t+t_{pump})}$ which means $\bar{\psi}_2$ approaches zero exponentially but never reaches it during finite amount of time. At time zero, the pump is removed and $\bar{\psi}_2$ reaches a small value

$$\bar{\psi}_{20}^2 = \frac{-\alpha_{2H}/2}{(1 - \alpha_{2H}/\alpha_{2L})} e^{4\alpha_{2H}\gamma_2 t_{pump}}. \quad (G2)$$

We first consider the fast cooling limit $t_m = 0$. After time zero, $\bar{\psi}_2$ goes back towards minimum II following the dynamics

$$\bar{\psi}_2^2(t) = \frac{\alpha_{2L}/2}{\left(\frac{\alpha_{2L}}{2\bar{\psi}_{20}^2} - 1\right)e^{-4\alpha_{2L}\gamma_2 t} + 1} \approx \bar{\psi}_{20}^2 e^{4\alpha_{2L}\gamma_2 t} \quad \text{for } 4\alpha_{2L}\gamma_2 t \ll \ln\left(\frac{\alpha_{2L}}{2\bar{\psi}_{20}^2}\right) \text{ and } \bar{\psi}_{20}^2 \ll \alpha_{2L}/2. \quad (G3)$$

Thus at time t_c when ψ_1 fluctuation crossovers to nonlinearity, $\bar{\psi}_2$ has recovered by an exponential factor. The more accurate picture for the probability distribution is that of Fig. 3(a) but shifted in ψ_2 direction by the amount of $\bar{\psi}_2^2(t_c)$. For the probability of trapping into phase I to be still close to one, we require that

$$\bar{\psi}_2^{2/\Delta}(t_c) \ll \langle \psi_1^2 \rangle_{t_c} \quad (\text{G4})$$

which yields

$$\psi_{20}^{2/\Delta} \ll \frac{\alpha_{1L}}{2} \zeta_1 (4\alpha_{1L}\gamma_1 t_c)^{-D/2} \quad (\text{G5})$$

and further leads to the criterion

$$t_{pump} \gg \frac{\Delta}{4|\alpha_{2H}|\gamma_2} \ln \frac{1}{\zeta_1} \equiv t_d \quad (\text{G6})$$

for the pump pulse in the leading order. Despite the logarithmic factor, this time scale can be made small with a larger $|\alpha_{2H}|$, i.e., a stronger pump will prepare the $\bar{\psi}_{20}$ with a smaller value at time zero.

If the cooling rate is finite, it is simpler to consider the case $t_m > t_{mu}$ such that the crossover happens at t_c before t_m . The pumping time is effectively longer than t_{pump} in this case since the suppression process of ψ_2 lasts until t_2 , when $\alpha_2(t)$ crosses zero. Applying Eq. (G4) to this case yields

$$t_{pump} \gg \frac{(\alpha_{2L} + |\alpha_{2H}|) t_m}{2|\alpha_{2H}|} \left(\sqrt{\frac{1}{2\gamma_1(\alpha_{1L} + |\alpha_{1H}|) t_m} \ln \frac{1}{\zeta_1} + \frac{|\alpha_{1H}|}{\alpha_{1L} + |\alpha_{1H}|}} \right) \\ \left(\sqrt{\frac{1}{2\gamma_1(\alpha_{1L} + |\alpha_{1H}|) t_m} \ln \frac{1}{\zeta_1} + \frac{|\alpha_{1H}|}{\alpha_{1L} + |\alpha_{1H}|}} - \frac{2|\alpha_{2H}|}{\alpha_{2L} + |\alpha_{2H}|} \right) \quad (\text{G7})$$

to leading order. For sufficiently large $|\alpha_{iH}|$, the right hand side of Eq. (G7) becomes negative and thus the criterion is satisfied by any $t_{pump} > 0$. This is because in the cooling process before t_2 , the high temperature stage already suppresses ψ_2 well enough.

In realistic situation, the pump might not be strong enough and the proportion of phase I domains created, p_1 , can be calculated as a function of pump fluence/duration. It should crossover sharply from 0 to 1 at the boundary of Eq. (G6) or Eq. (G7) depending on which regime the cooling rate is in.

Appendix H: Joint probability function

The probability that $\psi(0) = A$ and $\psi(r) = B$ is

$$P(A, B) = \mathcal{N} \int \mathcal{D}\psi \text{Exp} \left[-\sum_k D_k^{-1} \psi_k \psi_{-k} \right] \delta(\psi(0) - A) \delta(\psi(r) - B) \quad (\text{H1})$$

where

$$D_k = e^{4\alpha_k \gamma t} \frac{1}{\alpha_k} \frac{T}{E_c V} = 2 \langle \psi_k^2 \rangle_t \quad (\text{H2})$$

and \mathcal{N} is the normalization of the functional integral and δ is a functional delta function. Representing the delta functions by integrals gives

$$P(A, B) = \mathcal{N} \int d\lambda_1 d\lambda_2 \int \mathcal{D}\psi \text{Exp} \left[-\sum_k D_k^{-1} \psi_k \psi_{-k} + i\lambda_1 (\psi(0) - A) + i\lambda_2 (\psi(r) - B) \right] \quad (\text{H3})$$

or, Fourier transforming the real-space ψ

$$P(A, B) = \mathcal{N} \int d\lambda_1 d\lambda_2 \int \mathcal{D}\psi \text{Exp} \left[-\sum_k D_k^{-1} \psi_k \psi_{-k} + i \left(\lambda_1 + e^{ik \cdot r} \lambda_2 \right) \psi_k - i\lambda_1 A - i\lambda_2 B \right]. \quad (\text{H4})$$

We can now perform the integral over the ψ_k and arrive at

$$P(A, B) = \mathcal{N}' \int d\lambda_1 d\lambda_2 \text{Exp} \left[-\sum_k \frac{D_k}{4} (\lambda_1^2 + \lambda_2^2 + 2\cos(k \cdot r) \lambda_1 \lambda_2) - i\lambda_1 A - i\lambda_2 B \right] \quad (\text{H5})$$

The sum over k results in

$$P(A, B) = \mathcal{N}' \int d\lambda_1 d\lambda_2 \text{Exp} \left[-(\lambda_1, \lambda_2) \hat{M}(\lambda_1, \lambda_2)^T - i(\lambda_1 A + \lambda_2 B) \right] \quad (\text{H6})$$

where

$$\begin{aligned} \hat{M} &= \frac{1}{2} \begin{pmatrix} \langle \psi(0)^2 \rangle & \langle \psi(0)\psi(r) \rangle \\ \langle \psi(0)\psi(r) \rangle & \langle \psi(0)^2 \rangle \end{pmatrix} = \frac{1}{2} \frac{G}{2\alpha} \left(\frac{1}{16\pi\gamma t} \right)^{D/2} e^{4\alpha\gamma t} \begin{pmatrix} 1 & e^{-r^2/2\xi(t)^2} \\ e^{-r^2/2\xi(t)^2} & 1 \end{pmatrix} \\ &= \frac{\alpha_1}{4} \begin{pmatrix} 1 & e^{-r^2/2\xi(t_c)^2} \\ e^{-r^2/2\xi(t_c)^2} & 1 \end{pmatrix} \end{aligned} \quad (\text{H7})$$

at $t = t_c$. We finally perform the λ integrals, getting

$$\begin{aligned} P(A, B) &= \mathcal{N}' \frac{\pi}{\sqrt{\text{Det}[M]}} \text{Exp} \left[-\frac{1}{4} (A, B) \hat{M}^{-1} (A, B)^T \right] \\ &= \frac{1}{\pi} \frac{1/\alpha}{\sqrt{1 - e^{-r^2/2\xi(t_c)^2}}} \text{Exp} \left[-\frac{1/\alpha}{1 - e^{-r^2/2\xi(t_c)^2}} \begin{pmatrix} A & B \end{pmatrix} \begin{pmatrix} 1 & -e^{-r^2/2\xi(t_c)^2} \\ -e^{-r^2/2\xi(t_c)^2} & 1 \end{pmatrix} \begin{pmatrix} A \\ B \end{pmatrix} \right]. \end{aligned} \quad (\text{H8})$$

Appendix I: The coefficient λ and ϑ

The coefficients are:

$$\lambda = (c^2 - 4)^{(1/\Delta - 1)/2} \left(\frac{-2\alpha_1 + c\alpha_2}{(-2\alpha_2 + c\alpha_1)^{1/\Delta}} \right)^{1/2}, \quad (\text{I1})$$

and

$$\vartheta = \frac{2}{\pi} \lambda \Gamma \left[\frac{1}{2} (1 + 1/\Delta) \right] \alpha_1^{(1/\Delta - 1)/2} \Delta^{-D/(4\Delta)} \left(\frac{\alpha_1}{\alpha_2} \right)^{\frac{1}{2\Delta} (1 - D/2)} \left(\frac{\xi_{10}}{\xi_{20}} \right)^{D/(2\Delta)}. \quad (\text{I2})$$

Note that α_i should be interpreted as α_{iL} in the fast cooling limit.

Appendix J: Non-equilibrium phase diagrams

‘Nonequilibrium’ phase diagrams Fig. 10 can be drawn for α_{iH} . The system is originally at the blue dot α_{iL} . If the pump brings the α_{iH} to any of the colored regions, metastable trapping into the SC (I) state could happen. However, different regions have different stories as described in the main text. For example, if α_{iH} is in region 1 and $t_{\text{pump}} + t_0/2$ is much larger than $t_d = \frac{\Delta}{4|\alpha_{2H}|\gamma_2} \ln \frac{1}{\xi_1}$, the system can be brought to disordered state by the pump. The subsequent dynamics of fluctuation will lead the system into the metastable SC state if the relaxation in the SC direction is substantially faster.

Appendix K: Nano Granules

If the system is a nano granule whose size is smaller than a coherence length, one can neglect the spatial fluctuation and treat the order parameter as uniform, i.e., one could keep the $k = 0$ mode only. The initial dynamics is an expansion of the Gaussian probability due to thermal noise, regardless of the flow direction due to the potential. After the time $4\alpha\gamma t \sim 1$, the dynamics starts to be dominated by the flow. At this time, $\psi_i^2 \sim T_v/\alpha_i$ and is much smaller than α_i if the system volume V is not too small. Thus nonlinearity is not yet onset. After passing the crossover point $\psi_i^2 \sim T_v/\alpha_i$ to flow dynamics, the order parameter in each basin will be finally attracted to the corresponding minima, as shown in Fig. 4. One immediately observes that if ψ_i distribution is still tiny at the crossover point, most of the ψ lies inside basin I due to the nearly vertical shape of the basin boundary close to the origin.

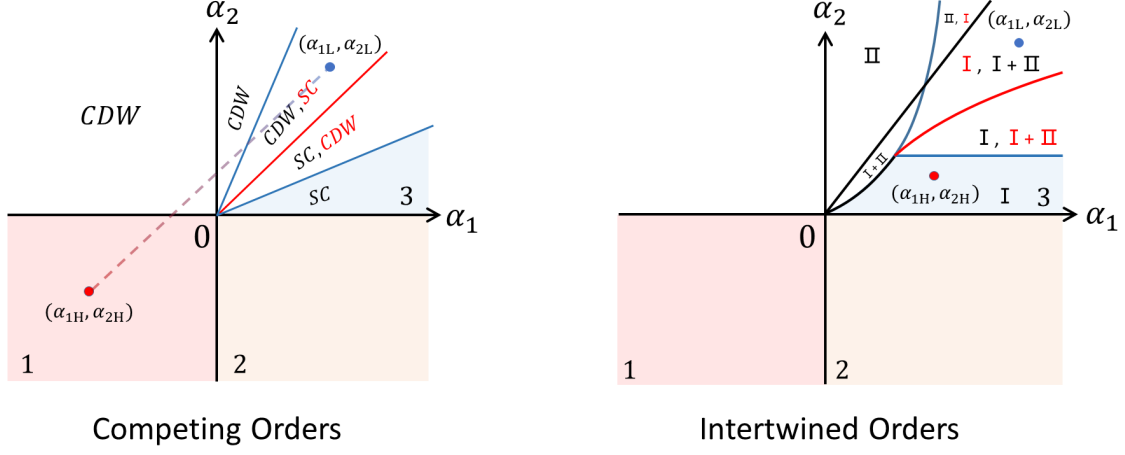


FIG. 10. Nonequilibrium phase diagram for the pumped parameter α_{iH} . If α_{iH} lies in the colored regions, as illustrated by the red dots, the system can be trapped into the metastable SC state. Dashed line is the trajectory of $\alpha_i(t)$ in the cooling process.

To estimate of probability of trapping into phase I , one can draw a rectangle centered at O with half lengths of $L_i = \sqrt{\langle \psi_i^2 \rangle}$. The length of its edge embedded in basin II is $l_2 = 4\lambda L_2^{\gamma_1 \alpha_1 / (\gamma_2 \alpha_2)}$ while the total length is $l = 4L_1 + 4L_2$. Therefore, the probability of trapping into phase I is roughly

$$p_1 \sim 1 - l_2/l = 1 - \kappa T_v^\delta. \quad (K1)$$

where $\delta = \frac{1}{2} (\gamma_1 \alpha_1 / (\gamma_2 \alpha_2) - 1) > 0$ and κ is order one. Since T_v is a very small number, this probability is almost unity. After trapped into it, the life time of this metastable state is exponentially large: $T_{life} \sim \frac{1}{\gamma} e^{U/T_v}$ where U is the dimensionless energy barrier between the global and metastable minima. The detailed calculation for the lifetime is described by Kramer's theory [35, 60].